



ADVANCED CONTROL AND CONDITION MONITORING PV SYSTEMS



Aalborg University
Institute of Energy Technology

FABRIZIO OLITA

Master Thesis

“ADVANCED CONTROL AND CONDITION MONITORING PV SYSTEMS”

Aalborg University
Institute of Energy Technology
Denmark, June 2012

Supervisors

Remus Teodorescu
Dzeso Sera
Sergiu Spataru

Fabrizio Olita
Project Group 1036

CONTENTS

1	INTRODUCTION.....	4
1.1	WHY PHOTOVOLTAIC TECHNOLOGY	4
1.2	BACKGROUND	5
1.2.1	PHOTOVOLTAIC TECHNOLOGY	5
1.2.2	PHOTOVOLTAIC SYSTEM TOPOLOGIES.....	6
1.2.3	INFLUENCE OF PARTIAL SHADOWS ON PV SYSTEMS	7
1.2.4	MAXIMUM POWER POINT TRACKING.....	9
1.3	PROJECT OBJECTIVES	11
1.4	LIMITATIONS.....	11
2	OVERVIEW OF PV MODEL AND CONTROL	12
2.1	PV MODEL.....	12
2.2	SYSTEM LAYOUT	14
2.3	P&O MPPT METHOD.....	16
3	MODEL REFERENCE ADAPTIVE SYSTEM.....	19
3.1	GENERAL OVERVIEW	19
3.2	MODEL REFERENCE PREDICTION AND SUPERVISION CONTROL	20
3.2.1	CHARACTERIZATION REFERENCE MODEL.....	20
3.2.2	PARAMETERS ESTIMATION	22
3.2.3	OBJECTIVE FUNCTION AND SUPERVISION CONTROL.....	23
3.3	APPLICATION AND SIMULATIONS.....	24
3.3.1	V-I CURVE MONITORING ALGORITHM CONTROL.....	24
3.3.2	PV PLANT CHARACTERISTICS AND SIMULATIONS.....	28
3.3.3	ADJUSTMENT PARAMETERS MECHANISM	35
4	CONCLUSION	38
	APPENDICES	39
A.	FINITE DIFFERENCE METHOD.....	39
B.	NEWTON-RAPHSON METHOD	41
C.	SIMULINK® SCHEMES.....	43
D.	MATLAB® CODE	46

1 INTRODUCTION

1.1 WHY PHOTOVOLTAIC TECHNOLOGY

Renewable energy is energy generated from renewable natural resources, such as solar radiation, wind, rainfall, tides, geothermal heat, etc. The photovoltaic solar energy (PV) is the most direct way to convert solar radiation into electricity and is based on the photovoltaic effect. The photovoltaic effect is a physical phenomenon of converting the energy carried by optical electromagnetic radiation into electrical energy. It was discovered by E. Becquerel in 1839, when he found that certain materials produce an electric current when exposed to light. The photovoltaic effect remained a laboratory curiosity from 1839 until 1959, when the first silicon solar cell was developed at Bell Laboratories in 1954. It already had an efficiency of 6%, which was rapidly increased to 10%. Practically all photovoltaic devices are made with solar cells of semiconductor material which has to be able to absorb a large part of the solar spectrum [1].

The main application has been in space vehicles for many years, instead terrestrial application of photovoltaic (PV) developed very slowly, nevertheless PV fascinated not only the researchers but also the general public.

Photovoltaic technology has the following major advantages and disadvantages [2, 3]

Some advantages can be:

- the energy source, the sun, is free, therefore it is sustainable and will never run out
- no pollution, it doesn't produce carbon dioxide
- no mechanical moving parts, no noise, direct conversion of solar radiation into electricity
- PV modules have a very long lifetime
- its power ranges from microwatts to megawatts.

Some disadvantages can be:

- toxic chemicals, like cadmium and arsenic, are used in the PV production process but these environmental impacts are minor and can be easily controlled through recycling and proper disposal
- solar energy is somewhat more expensive to produce than conventional sources of energy due in part to the cost of manufacturing PV devices and in part to the conversion efficiencies of the equipment
- solar power is a variable energy source, with energy production dependent on the sun
- solar facilities may produce no power at all some of the time, which could lead to an energy shortage if too much of a region's power comes from solar power.

Using renewable energy will be the key to tackle climate change as well as to achieve sustainable energy. To achieve the renewable energy target, more and more funds have been and will be invested in the research and development of the renewable energy and to derive affordable and efficient renewable energy is one of the main renewable energy research topics [4].

In these years photovoltaic market has had a fast increase since 2005 when the market was 5000MW to the 2008 with 15GW and in the 2010 with 40GW [2].

1.2 BACKGROUND

1.2.1 PHOTOVOLTAIC TECHNOLOGY

Sunlight is composed of packets of energy, called photons. The photon is the basic unit of light and other electromagnetic radiation. Photons contain various amount of energy corresponding to the different wavelengths of light [5, 6].

The energy can be expressed by the equation: $E = h \nu$, where h is Planck's constant and ν is the photon's frequency. As the wavelength of light increases, the photon energy of that light decreases. When certain materials, such as semiconductors, are exposed to light, the photons within a certain energy band can be absorbed, other photons may pass through the material or be reflected without being absorbed. Different semiconductors have different optical absorption coefficients [3, 7, 8].

When a photon is absorbed, the energy of the photon will be transferred to an electron of the material under illumination. When this energy is larger than the electron binding energy, the electron will be ejected from its ground energy state, and an electron-hole pair will be created. The holes and electrons are then separated by the electric field produced by the p-n junction, this results in a potential difference and a current flow (electricity) through an external circuit if the PV cell is connected to a load [1].

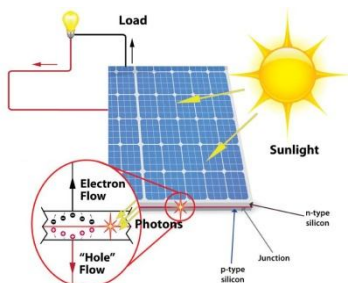


Figure 1.1a. Photovoltaic P-N junction exposed to light[9]

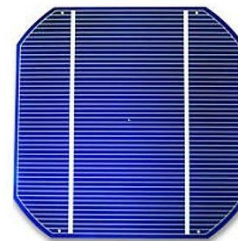


Figure 1.1b. Photovoltaic cell[10]

PV cells can be manufactured from different materials.

There are two major PV technologies: *wafer-based silicon* technology and *thin-film* technology. Crystalline silicon PV cells are more efficient than thin-film ones but more expensive to produce. They are most commonly used in medium to large electrical applications such as grid connected PV generators. Mono-crystalline and poly-crystalline (or multi-crystalline) are two dominant silicon technologies [3, 6]

Mono-crystalline PV cells use pure semiconducting materials and have higher efficiency. As the second generation PV cell technology, thin-film PV cells use very thin layers of semiconducting materials, so they can be manufactured in large quantity at low cost. However, the efficiency is lower. Currently, this technology prevails in small consumer applications such as watches, calculators and toys. In addition to the above technologies, there are some other PV technologies

are developing as Hybrid PV cells combine both mono-crystalline and thin-film silicon to produce cells with the best features of both technologies [1, 11].

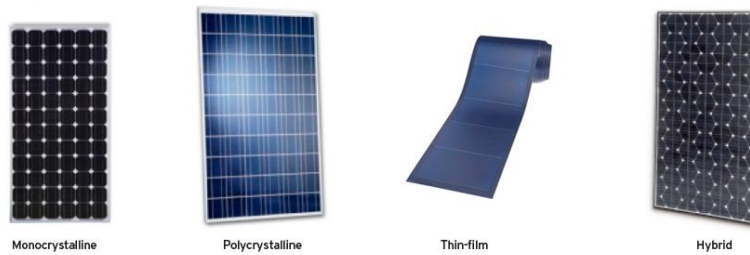


Figure 1.2. Wafer-based silicon technology, thin-film technology and hybrid technology[12-14]

The solar cell described above is the basic building block of the PV power system. Typically, it is a few square inches in size and produces about one watt of power. For obtaining high power, numerous such cells are connected in series and parallel circuits on a panel (module) area of several square feet, Figure 1.3. The solar array is defined as a group of several modules electrically connected in series-parallel combinations to generate the required current and voltage.

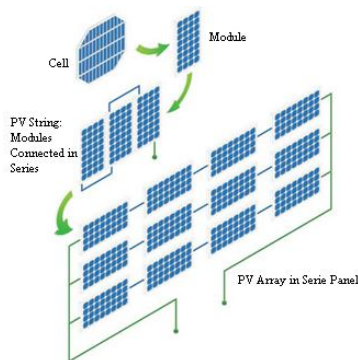


Figure 1.3 Cell interconnection[15]



Figure 1.4. Example of PV array[16]

1.2.2 PHOTOVOLTAIC SYSTEM TOPOLOGIES

There are two types of PV systems: *stand-alone system* and *grid connected system*.

Stand-alone photovoltaic powered systems with peak PV powers can have from milliwatts to several kilowatts. They do not have a connection to an electricity grid. In order to ensure the supply of the stand-alone system with electric power also in the times without radiation or with very low radiation, stand-alone systems mostly have an integrated storage system. If the systems are used only during the time when the radiation is sufficient to supply the system with electric power directly, a storage system is not necessary. This also applies to the situation in which the product delivered by the system can be stored.

At present, a very great variety of stand-alone systems exist. Examples range from solar calculators and watches to systems for traffic control to systems that are able to supply one or several buildings in remote areas with electric power. They can be DC systems with or without a storage battery, or they can be AC systems with an inverter.

Grid-connected PV systems always have a connection to the public electricity grid via a suitable inverter because a PV module delivers only dc power.

Normally there are almost no effects of the PV systems on the grid affecting power quality, load-on lines, and transformers, etc. However, for a larger share of PV in low-voltage grids, as in solar settlements, these aspects need to be taken into account. From a technical point of view, there will be no difficulty in integrating as much PV into low-voltage grids as the peak load of the respective segment decentralized grid-connected PV systems, central grid-connected PV systems [1, 11].

Decentralized grid-connected PV systems have mostly a small power range and are installed on the roof of buildings (flat-roof installation) or integrated into building facades

Central grid-connected PV systems have an installed power up to the MW range. With such central photovoltaic power stations it is possible to feed directly into the medium or high voltage grid [4].

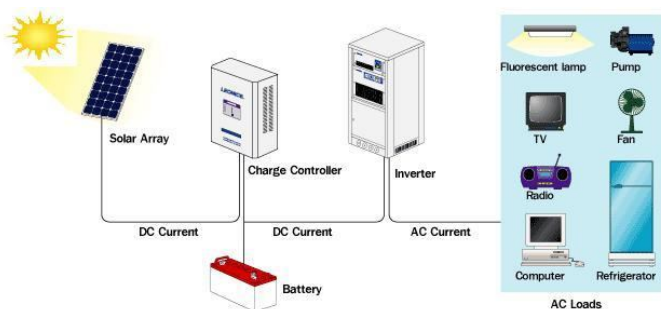


Figure 1.5. Stand alone system[17]

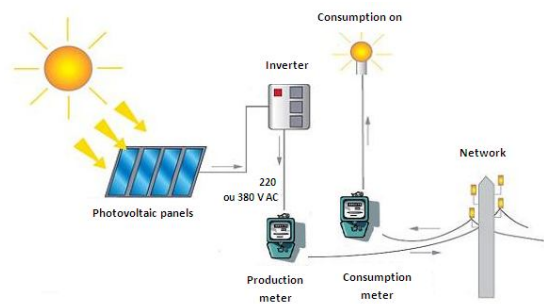


Figure 1.6. Residential grid connected system[18]

1.2.3 INFLUENCE OF PARTIAL SHADOWS ON PV SYSTEMS

Ideally PV modules should be built using identical cells so to have a module with uniform characteristic. We see the solar cell behaves like a current source, that is, if irradiation cannot reach the p-n junction of a particular solar cell – due to shadowing, dirt, snow and leaves – then the photon current I_{ph} of this particular solar cell is zero or very small [19, 20].

When connecting PV cells/modules in series, if one of the PV cells/modules has a much lower photo current I_{ph} than others due to partial shading, dust or degradation, it operates as a load for other cells and is reversed biased. This cell/module will then dissipate energy rather than generate hence leading to a cell temperature rise and if the temperature is too high the cell/module can be damaged and affect the whole PV module/array is compromised [8].

The most common method to avoid this is to put a bypass diode across a PV string or modules, as shown in Figure 1.7. These bypass diodes permit that the particular solar cell, which cannot conduct current, is bridged-over and the photon current of the remaining solar cells of a string can flow. The number of bypass diodes per module is a compromise between avoiding the formation of hot spots and the costs for extra components. Today, for crystalline silicon PV modules, the optimized number of cells in series per bypass diode is commonly 18 [21].

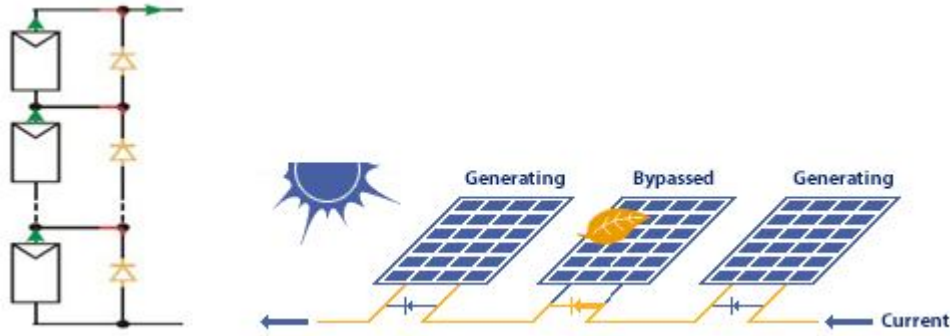


Figure 1.7. PV modules with bypass diodes[22, 23]

As described in the previous section, bypass diodes are usually used in PV modules to protect them from hot-spot damage. Because the shaded cell defines the current of the entire series string, even minor shading could cause a major reduction in power output of PV modules.

In [24] characteristics of PV string under partial shaded conditions are studied and in particular an array with 3 cells is considered as showed in Figure 1.8.

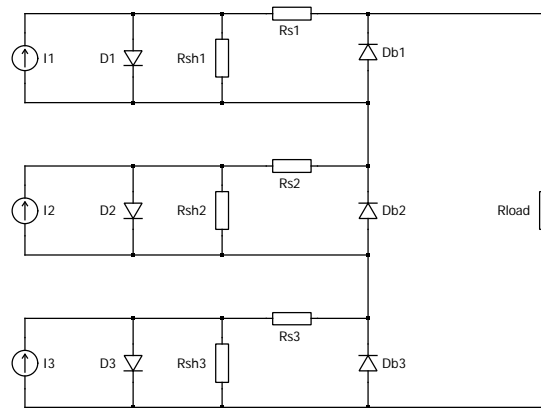


Figure 1.8. Electric circuit of three panels connected in series with bypass diodes

I_1 , I_2 and I_3 are currents, proportional to the irradiation received by each cell; Db_1 , Db_2 and Db_3 are bypass diodes. The irradiation has left on the first panel be high, on the second panel be medium and on the third panel be low: $I_1 > I_2 > I_3$.

A portion of power from highly illuminated panels, instead of getting wasted in low illuminated panels will be available to the load. Low illuminated panels however make no contribution to the load power as these are short circuited by the bypass diodes.

Figure 1.9 shows the characteristic of photovoltaic string with bypass diodes under non uniform irradiation and it shows how the bypass diodes introduce multiple peaks in the characteristics.

The irradiation level considered in the experiment is of 1000 W/m^2 at the temperature of 25°C .

The shading effect is artificially generated such that cells receive irradiation levels of $G_1=100\%$, $G_2=60\%$ and $G_3=20\%$ respectively.

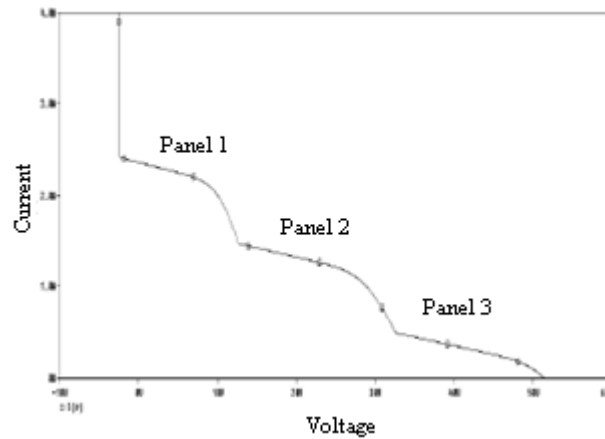


Figure 1.9. I-V characteristics of PV array under partial shaded condition [24]

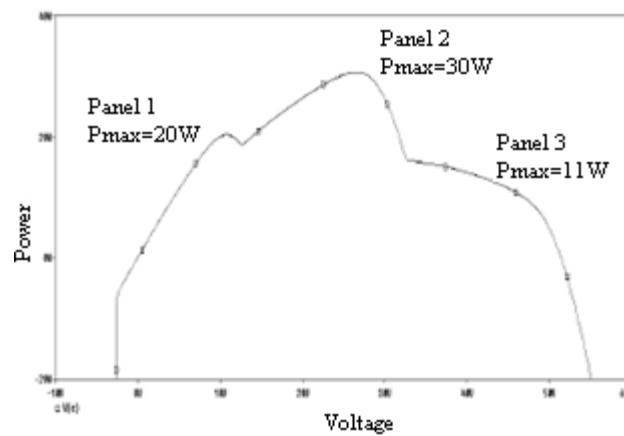


Figure 1.10 P-V characteristics of PV array under partial shaded condition [24]

In conclusion in a photovoltaic array non-uniform irradiation can damage poorly illuminated cells.

A large proportion of electrical power generated by highly illuminated cells is wasted as heat in poorly illuminated cells, so the use of bypass diodes can save the poorly illuminated panels from damage and also make this energy available to the load.

P-V characteristics under non uniform irradiation with bypass diodes is shown in Figure 1.10 and contains multiple peaks that is more local maximum points and the magnitude of the global maxima is dependent on the array configuration and shading patterns.

The partial shadow condition, anyway, influence considerably the PV system performance, reducing the output power even in presence of bypass diode, that isn't used to avoid it, for that reason a partial shadow detection is desirable, for monitoring the system and as far as possible to preview a future partial shadowing on all the system or on a part of it.

1.2.4 MAXIMUM POWER POINT TRACKING

Photovoltaic (PV) array under uniform irradiance exhibits a voltage-current characteristic with an unique point, called the maximum power point (MPP), where the array produces maximum

output power [25]. It is always essential to track maximum power from photovoltaic sources. Failure to track the global maximum power point under partial shading conditions is one of the major reasons that lead to significant power losses. Several maximum power point tracking methods have been proposed to deal with this problem[24, 26, 27]. In Figure 1.11 an example of PV module characteristics in terms of P-V and V-I, for different irradiance levels and different temperature values (without partial shadow) are shown. The MPP point has been also marked in both figures.

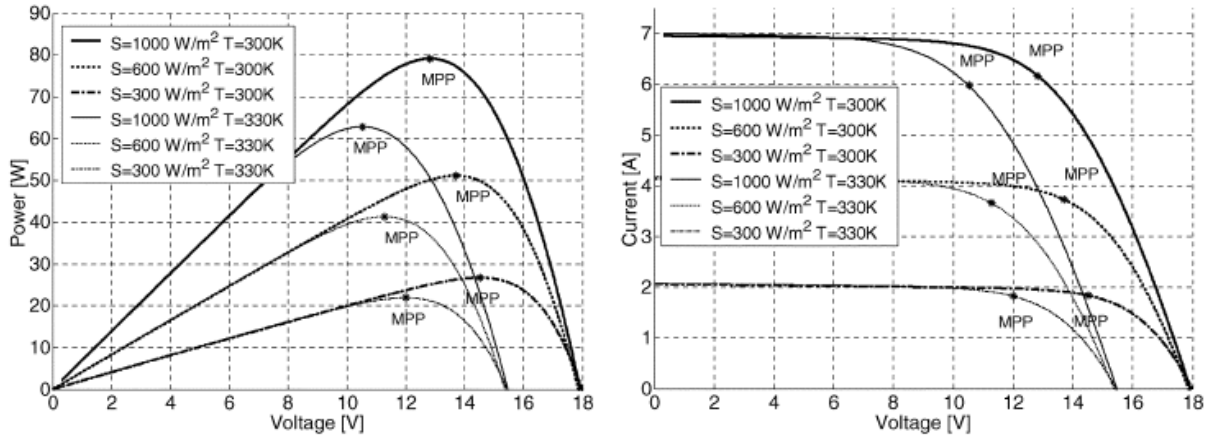


Figure 1.11. PV power and current characteristics for three irradiance levels and two different temperature [25]

As evidenced in Figure 1.11, since the V-I characteristic of a PV array, and hence its MPP, changes as a consequence of the variation of the irradiance level and of the panels' temperature, (which is in turn function of the irradiance level, of the ambient temperature, of the efficiency of the heat exchange mechanism and of the operating point of the panels), it is necessary to track continuously the MPP in order to maximize the power output from a PV system, for a given set of operating conditions.

Maximum Power Point Tracking (MPPT) is important in solar power systems because it reduces the solar array cost by decreasing the number of solar panels needed to obtain the desired output power. Several different MPPT methods have been proposed, and in [28] there has been comprehensive experimental comparison between different algorithms and their overall Maximum Power Point (MPP) tracking efficiencies under varying conditions (i.e. illumination, temperature, and load).

One significant problem in PV systems is the probable mismatch between the operating characteristics of the load and the PV array.

When a PV array is directly connected to a load, the system's operating point will be at the intersection of the V-I curves of the PV array and load. Under most conditions, this operating point is not at the PV array's maximum power point (MPP). To overcome this problem, an MPPT can be used to maintain the PV array's operating point at the MPP. However, the location of the MPP in the V-I plane is not known a priori. It can be calculated using a model of the PV array and measurements of irradiance and array temperature, but making such measurements is usually too expensive for this application, and often the required parameters for the PV array model are not known adequately. Thus, the maximum power point algorithm must continuously search for the MPP. Several MPPT search algorithms have been proposed that make use of different characteristics of solar panels and the location of the MPP.

In [28] as we said, three most important strategies are compared: P&O (Perturb and Observe), INC (Incremental Conductance) and CV (Constant Voltage).

Analysis shows that good results are obtained with the first and second strategy, instead although incremental conductance is able to provide marginally better performance, the increased complexity of the algorithm will require more expensive hardware, and therefore may have an advantage over perturb and observe only in large PV arrays.

In 2.3 we are going to describe the P&O method considering advantages and disadvantages.

1.3 PROJECT OBJECTIVES

In the present work, we want to focus our attention on the advanced control for condition monitoring of a PV system. In accordance with the need to maximize the energy output of PV systems, the project has two main objectives:

- to propose a strategy based on the predictive reference control, in order to supply a priori an estimation of current and establish, with a algorithm control, if system is working in total irradiance condition or in shadowing condition.
- to test a strategy for adjustment parameters for reference model.

1.4 LIMITATIONS

Although there is a large number of PV inverter topologies present in the literature and on the market, only a single-stage topology is considered here.

Other limitations will be applied on the plant, considering:

- 120 W multicrystalline photovoltaic module (MSX 120)
- Four parameter PV model
- Single-phase inverter topology
- P&O MPPT method
- A smooth voltage-current curve of the plant

2 OVERVIEW OF PV MODEL AND CONTROL

2.1 PV MODEL

Generally some electrical equivalent circuits derived from the physical mechanism of PV cells are accepted [4, 11] and different model we can consider to describe a PV module, but more parameters we consider, more the model is difficult to study.

The most simple solar cell equivalent circuit is shown in Figure 2.1 from which the nonlinear voltage–current curve of the equivalent solar cell, can be obtained through numerical simulation.

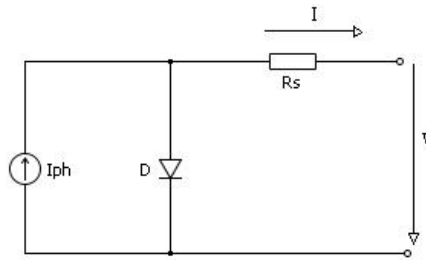


Figure 2.1. Equivalent circuit of a PV cell

The mathematical model of current in function of voltage is given by non linear equation:

$$I = I_{ph} - I_o \left(e^{\frac{V + I R_s}{V_t}} - 1 \right) \quad (2.1)$$

$$V_t = \frac{A k T}{q} \quad (2.2)$$

Where:

- V – PV cell terminal voltage (V)
- I – PV cell terminal current (A)
- V_t – PV cell thermal voltage (V)
- I_{ph} – photocurrent (A)
- I_o – dark saturation current (A)
- R_s – cell series resistance (Ω)
- A – p-n junction ideality factor
- q – electronic charge = 1.6×10^{-19} (C)
- k – Boltzmann's constant = 1.38×10^{-23} (J/K)

T – junction temperature (K)

There are 4 salient parameters to define the shape of the V-I curve described by the model above: I_{ph} , I_o , V_t , R_s , obtained solving conditions at open circuit and short circuit such as equations in [4].

The characteristic curve $I(V)$ is showed in Figure 2.2 with blue line , instead the power curve $P(V)$ is showed with red line.

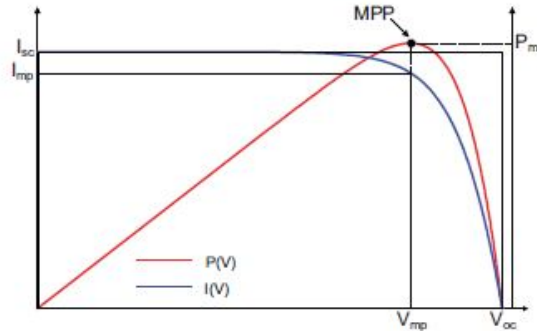


Figure 2.2. Characteristics $I(V)$ and $P(V)$ curves

The Maximum Power Point (MPP) is an important point because the array produces maximum output power in it and it's such to fulfill the condition:

$$\frac{dP}{dV} = 0 \quad (2.3)$$

in correspondent of current and voltage I_{mp} and V_{mp} :

$$I_{mp} = I_{ph} - I_o \left(e^{\frac{V_{mp} + I_{mp} R_s}{V_t}} - 1 \right) \quad (2.4)$$

As said above-mentioned in 1.2.4 , the array, under uniform irradiance, exhibits an unique point, instead when a PV array is under partial shading conditions, its characteristic may exhibit multiple maximum power points.

Other important parameters are the Fill Factor, given by:

$$FF = \frac{V_{mp} I_{mp}}{V_{oc} I_{sc}} \quad (2.5)$$

and the efficiency given by:

$$\eta = \frac{V_{mp} I_{mp}}{P_{in}} \quad (2.6)$$

The following figures show how efficiency changes under influence of temperature and irradiance. In Figure 2.3 the PV cell (or module) with low R_s , the efficiency increases with irradiance and decreases with increasing temperature.

Instead in Figure 2.4 the PV cell (or module) with high R_s , the efficiency decreases with increasing both irradiance and temperature.

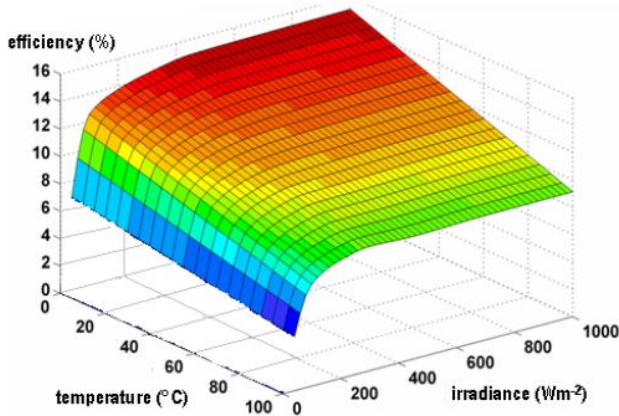


Figure 2.3. PV cell (module) with low R_s [29]

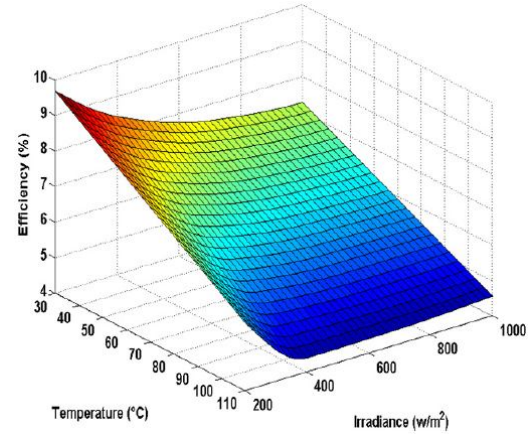


Figure 2.4. PV cell (module) with high R_s [29]

The output voltage is usually too small for most applications, therefore, to produce useful DC voltage, a number of PV cells are connected in series and mounted in a support frame, which forms a PV module (or a PV panel), at the same way to generate higher current PV modules can be connected in parallel to form a PV array for higher power applications.

If there are N_s cells connected in series and N_p parallel strings in the array, voltage and current are given by (2.7) and (2.8):

$$V_{dc} = N_s V \quad (2.7)$$

$$I_{dc} = N_p I \quad (2.8)$$

2.2 SYSTEM LAYOUT

To harness photovoltaic energy, different intermediate conversion stages and control structures have to be considered. In this paragraph we will deal briefly with the control system.

In Figure 2.5 and 2.6 a typical photovoltaic structure is shown, where the first block, PV string, is composed by photovoltaic panels as described in section 1.2.1, instead the last block is just a residential connection grid.

The intermediate stages preview different conversion topologies. Typical structures for residential application are: the *Multi-string inverter* where each string has its own boost dc/dc and all outputs are connected with just one inverter dc/ac block; the *String inverter* or *Module inverter* where each string or module has just its own inverter dc/ac block.

Some advantages of AC module are: each module works independently; high modularity allowing

easy system expansion; use of standard AC installation material which reduces costs of installation material and system design; no mismatch losses at system level as each AC module operates in its own Maximum Power Point (MPP).

All these topologies can preview a transformer stage or not, today more than 70% of the PV inverters sold on the market are transformer-less achieving 98% max conversion efficiency [29].

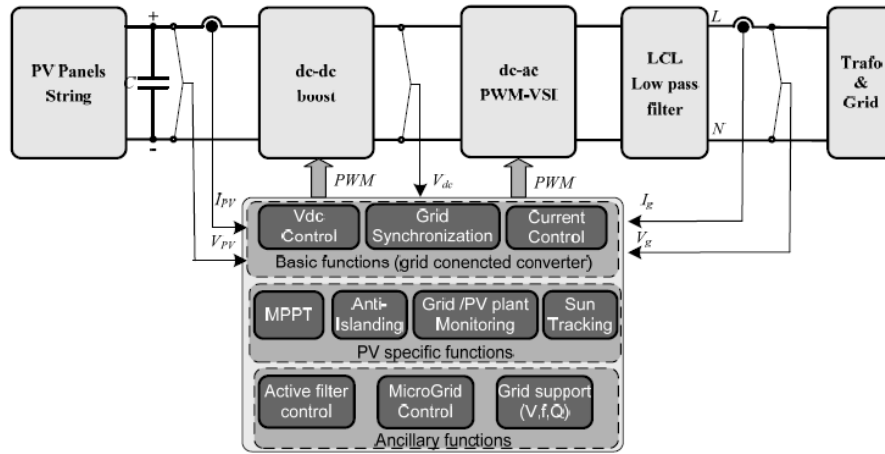


Figure 2.5. Two stages photovoltaic conversion structure [29]

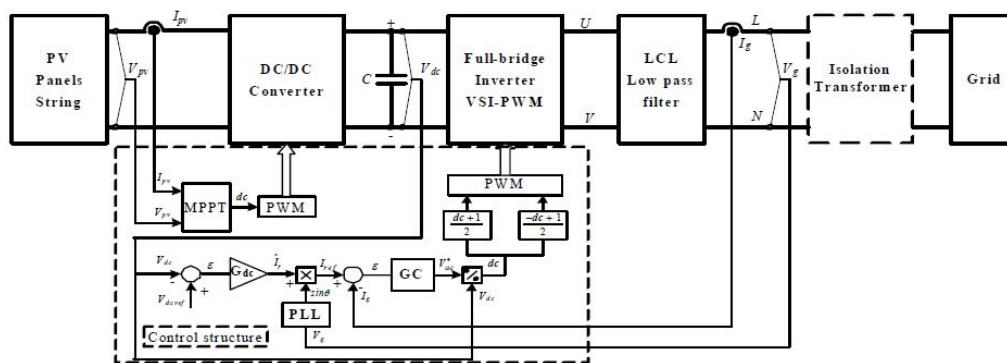


Figure 2.6. Control scheme for two stages structure [29]

In Figure 2.5 and 2.6 we can see different blocks of conversion structure and the control block structure with all its functions. In Figure 2.7 the photovoltaic conversion electrical circuit is shown, composed by a first stage with a boost dc/dc converter, a second stage with a half-bridge or full-bridge inverter dc/ac and third stage with a LCL low pass filter.

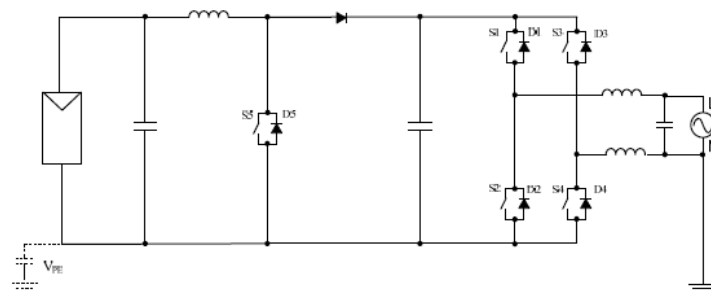


Figure 2.7. Two stages photovoltaic conversion electrical circuit [29]

An alternative solution could be the use of a single-stage converter where the dc/dc converter is avoided and in order to ensure the necessary dc voltage level the PV array can be a string of PV panel or a multitude of parallel strings of PV panels.

The disadvantages of the single-stage converter are is the narrower voltage range in which they can work.

In Figures 2.8 and 2.9 the control scheme for single stage structure and relative electrical circuit are reported.

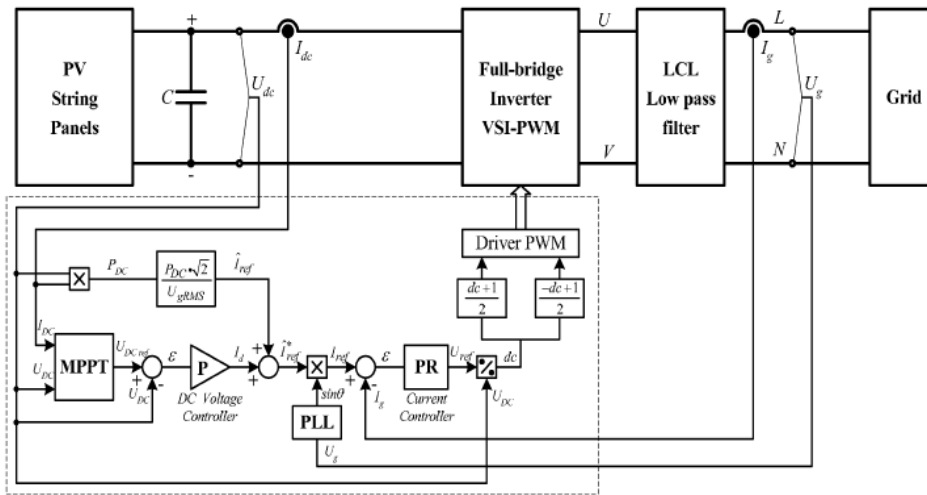


Figure 2.8. Control scheme for single stage structure [29]

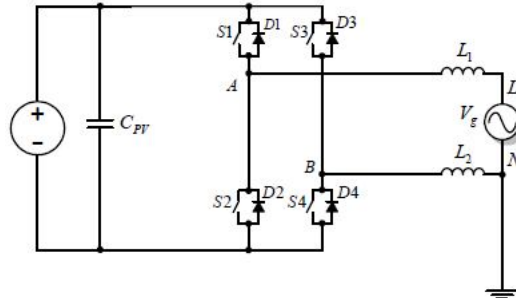


Figure 2.9. Single stages photovoltaic conversion electrical circuit [29]

2.3 P&O MPPT METHOD

The perturb and observe (P&O) method is the most popular MPPT algorithm today [30]. As describe in 1.2.4, it consists to find the maximum power expressed in (2.3), for which the numerical derive is satisfied:

$$P_k - P_{k-1} = 0 \quad (2.9)$$

Following the power curve the algorithm lets the voltage increases or decrease until max power point is found.

If the operating voltage of the PV array is perturbed in a given direction and if the power drawn from the PV array increases, this means that the operating point has moved toward the MPP and, therefore, the operating voltage must be further perturbed in the same direction. Otherwise, if the power drawn from the PV array decreases, the operating point has moved away from the MPP and, therefore, the direction of the operating voltage perturbation must be reversed [28].

Advantages of this method are:

- the simplicity
- the low computational demand
- it is applicable for generic systems.

Disadvantages are:

- the tradeoff between speed and accuracy
- the possibility to track in wrong way during fast changing conditions.

A drawback of P&O MPPT technique is that, at steady state, the operating point oscillates around the MPP giving rise to the waste of some amount of available energy [25, 26, 29].

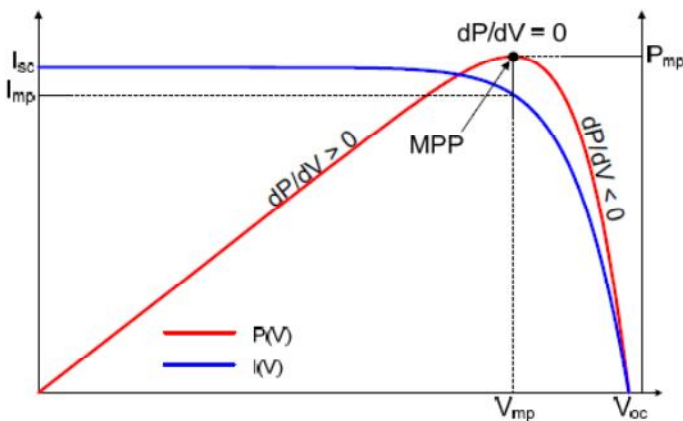


Figure 2.10. Power curve and MPP[29]

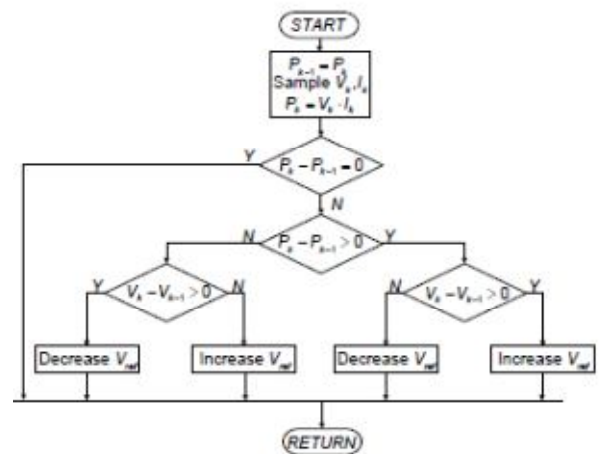


Figure 2.11. P&O MPPT method[29]

If the change of power caused by environmental change within one MPPT perturbation period is larger than the change of power caused by the MPPT perturbation, the tracker gets confused [29].

In order to improve speed while maintaining steady-state oscillations low, many strategies are researched and applied [28, 31].

In [25], for example, the P&O MPPT parameters are customized in order to limit the negative effects associated to the above drawbacks.

The key idea underlying the proposed optimization approach lies in the customization of the P&O MPPT parameters to the dynamic behavior of the whole system composed by the specific converter and PV array adopted.

The amplitude of the duty cycle perturbation is one of the two parameters requiring optimization: lowering the amplitude of duty cycle, reduces the steady-state losses caused by the oscillation of the

array operating point around the MPP; however, it makes the algorithm less efficient in case of rapidly changing atmospheric conditions.

The sampling interval, that is the second parameter requiring optimization, should be set higher than a proper threshold in order to avoid instability of the MPPT algorithm and to reduce the number of oscillations around the MPP in steady state. In fact, considering a fixed PV array MPP, if the algorithm samples the array voltage and current too quickly, it is subjected to possible mistakes caused by the transient behavior of the whole system (PV array + converter), thus missing, even if temporarily, the current MPP of the PV array, which is in steady-state operation. As a consequence, the energy efficiency decays as the algorithm can be confused and the operating point can become unstable. To avoid this, it must be ensured that, after each duty-cycle perturbation, the system reaches the steady-state before the next measurement of array voltage and current is done [26].

We have seen how the most used MPPT algorithm works, and we have seen which are advantages and disadvantages, and many different strategies are applied.

3 MODEL REFERENCE ADAPTIVE SYSTEM

3.1 GENERAL OVERVIEW

With term *to adapt* we mean to change a behavior to conform to circumstances [32].

An adaptive system can be thought having two loops, one loop is a normal feedback with the process and its controller, the other loop is the adjustment parameters loop.

The model-reference adaptive system (MRAS) is an important adaptive control in which the desired performance is expressed in terms of reference model, which gives the desired response to a command signal [32] and its parameters are changed on the basis of feedback from the error, which is the difference between the output of the reference model and the output of the system.

The *plant* is assumed to have a known structure, although the parameters are unknown. For linear plants, this means that the number of poles and the number of zeros are assumed to be known, but that the locations of these poles and zeros are not, instead for nonlinear plants, this implies that the structure of the dynamic equations is known, but some parameters are not [33].

A *reference model* is used to specify the ideal response of system to the external command. Intuitively, it provides the ideal plant response which the adaptation mechanism should seek in adjusting the parameters. The choice of the reference model is part of the adaptive system design and this choice has to satisfy two requirements: it should reflect the performance specification in the control tasks, on the other hand this ideal behavior should be achievable for the adaptive control system [33].

The *adaptation* mechanism is used to adjust the parameters in the reference model, in MRAS systems the adaptation law searches parameters such that the response of the plant under control becomes the same as that of the reference model, the objective of the adaptation is to make the tracking error converges to zero. The main issue in adaptation design is to synthesize an adaptation mechanism which will guarantee the system remains stable and the tracking error converges to zero as the parameters are varied. Many formalisms in nonlinear control can be used to study the stability, such as Lyapunov theory and passivity theory, and to find adaptive control law for non linear systems, but this is a difficult problem because no general design methods are available, there is however much interest in adaptive control of non linear systems. Unfortunately there is no collection that can be called a theory of adaptive control in the sense specified. There is instead a scattered body of results, which gives only partial results. One reason for this is that the behavior of adaptive systems is quite complex because of their time-varying and non linear character [32].

With the term *to predict* instead, we mean to estimate the system output considering a model of it and to apply a control law such that the predicted output would be the same of reference [34]. Several ways to achieve predictive control have been suggested in the literature [32, 34]. Predictive

control algorithms are based on an assumed model of the process and on an assumed scenario for the future control signals. One basic idea in the predictive control algorithm is to rewrite the process model to get an explicit expression for the output at a future time [32].

In our adaptive system, we want to consider a reference model of a photovoltaic plant which parameters change in relation with characteristics of the process and its environment and for optimizing operation we propose to achieve a possible output current prediction.

The goal of *supervision control* is to maximize the power, it means that central controller receives the current of the reference model and current of the plant so to minimize the error between them represented as objective function, in correspondent of current error, an adjust signal is applied on adjustment parameters block.

In Figure 3.1 the advanced control general scheme is shown.

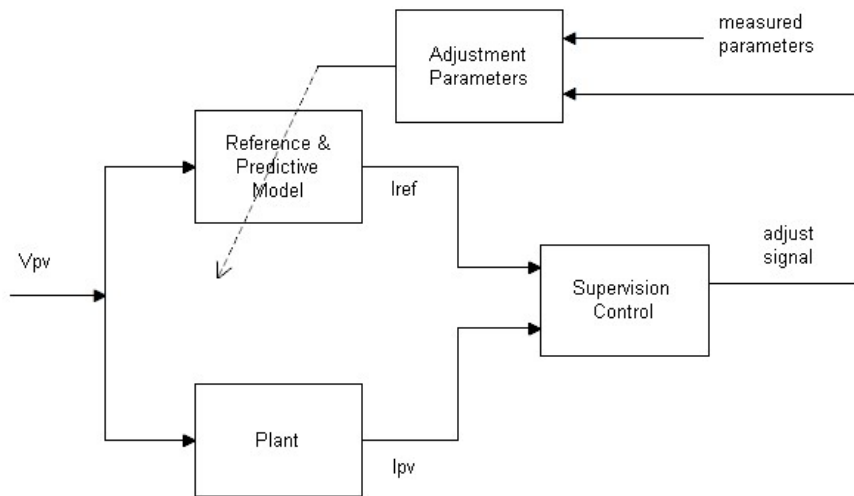


Figure 3.1. Advanced control general scheme

3.2 MODEL REFERENCE PREDICTION AND SUPERVISION CONTROL

The construction of an adaptive and predictive control contains the following steps:

- Characterization reference model
- Parameters estimation and adjustment parameters mechanism
- Object function and realization supervision control algorithm

3.2.1 CHARACTERIZATION REFERENCE MODEL

Let's begin describing different blocks showed in Figure 3.1 to apply to our PV system, describing step by step all basic models we need.

The *Plant* is represented by a single-stage photovoltaic structure, as shown in Figure 2.8, it includes a PV array (ref. section 2.1) composed by 16 panels in series and the P&O algorithm for MPPT (ref. section 2.3). The plant output I_{PV} is taken in correspondence of current I_{dc} in Figure 2.8.

The *reference and predictive model* block includes the ideal mathematical model of PV system and on it a reference current prediction is done.

Many models have been developed in literature [29], models with four, five or more parameters, in correspondence of a better precision we need. For simplicity and to determinate an analytic solution for parameters, our reference model will be based on the typical *four-parameter model*, function of voltage given by non linear equation reported in (2.1). When there is parameter uncertainty in a dynamic system (linear or nonlinear), one way to reduce it, is to use parameter estimation, inferring the values of the parameters from the measurements of input and output signals of the system. Parameter estimation can be done either online or offline. Offline estimation may be preferable if the parameters are constant and there is sufficient time, instead for estimation for parameters which vary (even though slowly) during operation, online parameter estimation is necessary to keep track of the parameter values [33]. Online determination of process parameters is a key element in adaptive control. A recursive parameter estimator can appears explicitly as a component in a model reference adaptive system. It is useful to view parameter estimator in a broad context of system identification. Since system identification is executed automatically in adaptive system, it is essential to have a good understanding of all aspects of the problem [32]. Assume that the parameter vector is unknown one can predict the value of the output based on the parameter estimate and the model.

The difference between the predicted output and the measured output is called the *prediction error* [33], but considering that the PV system is a strongly non linear system, to apply prediction error based estimation methods, is very difficult.

Let's write our PV system in a general form:

$$I=f(I_{ph},I_o,R_s,V_t,V_{PV},\pi) \quad (3.1)$$

where π represents all unknown behavior and that will not consider in our reference model.

The reference model is reported as follow:

$$\hat{I}=f(\hat{I}_{ph},\hat{I}_o,\hat{R}_s,\hat{V}_t,V_{PV}) \quad (3.2)$$

Considering we want to maximize the output power of PV system, we have to consider as input signal the reference voltage given by the plant (Figure 2.8), in this way our reference model can be rewritten as:

$$\hat{I}=\hat{I}_{ph}-\hat{I}_o(e^{\frac{V_{PV}+\hat{I}\hat{R}_s}{\hat{V}_t}}-1) \quad (3.3)$$

With $\hat{\cdot}$, we have indicated the estimated parameters of the reference model.

The prediction error is defined as the difference between the predicted output and the measured output, this parameter will be used for photovoltaic array monitoring condition.

$$\varepsilon=|\hat{I}-I| \quad (3.4)$$

3.2.2 PARAMETERS ESTIMATION

The development and the continued evolution of photovoltaics for electric power demands a deep knowledge of the interior characteristic measurements of PV cells, different algorithms are developed for PV parameters identification due to complex no linear mathematical model that can preview until seven parameters included in it [29, 35, 36].

Accurate modeling of PV modules requires a large number of training data consisting of a wide range of environmental conditions [36].

In this paragraph we want to present a simple way to estimate parameters of PV model, this method is based on the knowledge of datasheets of the PV system in standard test condition (STC).

As proposed in [37] and in [29], one can write expressions to determine the characteristic parameters under changing environment conditions, where G indicates irradiance and T temperature in which STC are respectively :

$$G_{stc} = 1000 \frac{W}{m^2} \quad (3.5)$$

$$T_{stc} = 298 \text{ K} \quad (3.6)$$

Let's report now the system of four equations in four parameters, already explained in 2.1, necessary to reference model to determinate the predictive behavior in nominal condition.

$$\left\{ \begin{array}{l} I_{sc} = I_{ph} \\ I_o = I_{sc} \exp\left(-\frac{V_{oc}}{V_t}\right) \\ V_t = \frac{2(V_{mp} - V_{oc})(I_{sc} - I_{mp})}{I_{mp} - (I_{sc} - I_{mp}) \log\left(\frac{I_{sc} - I_{mp}}{I_{sc}}\right)} \\ R_s = \frac{\left[V_{oc} - V_{mp} + V_t \log\left(\frac{(I_{sc} - I_{mp})}{I_{sc}}\right)\right]}{I_{mp}} \end{array} \right. \quad (3.7)$$

Where I_{sc} and V_{oc} reported in equations are respectively given by equations (3.8) and (3.9), with k_i the current temperature coefficient and K_v the voltage temperature coefficient:

$$I_{sc} = I_{sc_stc} \frac{G}{G_{stc}} + k_i (T - T_{stc}) \quad (3.8)$$

$$V_{oc} = V_{oc_stc} + K_v (T - T_{stc}) \quad (3.9)$$

3.2.3 OBJECTIVE FUNCTION AND SUPERVISION CONTROL

The supervision control compares instant for instant, the current I_{PV} of the PV system with the estimated current of calculate using the reference model, denoted as I_{ref} , so on one hand performing PV monitoring functions, and on the other hand it feeds back information needed to minimize the objective function and to correct to reference model parameters.

The objective function is to minimize the current error.

$$\min \varepsilon [I_{ref}, I_{PV}] \quad (3.10)$$

In Figure 3.2 the supervision algorithm control is proposed, which will be described above.

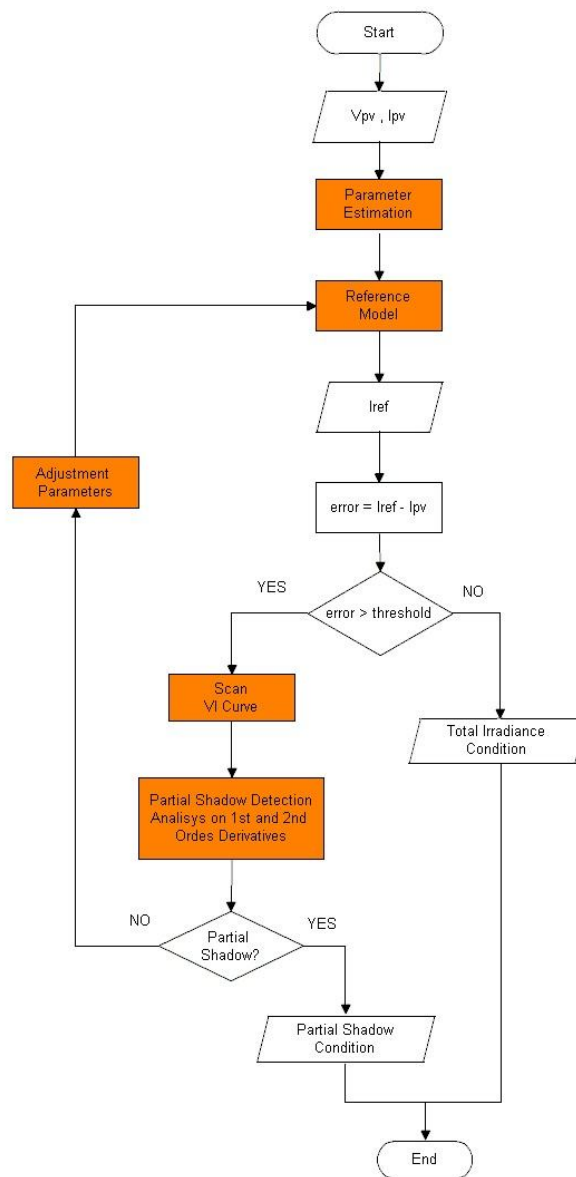


Figure 3.2. Supervision algorithm control

In the first steps, voltage V_{PV} and current I_{PV} are measured on the PV plant and the parameters are estimated as in (3.7), all these data will be useful for determination of reference model, as widely explained and reported in equations (3.3).

In the next step, the difference between reference current and PV current is achieved to observe how much the PV behavior differs from the estimated current in nominal condition. If the error is smaller than a threshold value then we can consider PV is working in normal condition of total irradiation, instead if the error is greater than the threshold, a monitoring algorithm control will run to observe if PV array is working under partial shadow condition. The monitoring algorithm control is based on analysis of the first and second derivatives, to study the PV curve shape. If algorithm reports a partial shadow condition, a message will be shown (Figure 3.35) to communicate the not total irradiance on PV caused by shadow.

On the other hand, it's possible that the error is greater than threshold but PV is not working in partial shadow condition, in this case the supervision control will provide to correct parameters through the adjustment parameters system.

In the next paragraph the V-I curve monitoring algorithm control and adjustment parameters mechanism will be reported.

3.3 APPLICATION AND SIMULATIONS

3.3.1 V-I CURVE MONITORING ALGORITHM CONTROL

In this paragraph we want to propose a V-I curve monitoring algorithm control, while in the next paragraph simulation results will be shown.

The monitoring algorithm control determinates if the PV system is working in partial shadow condition or not, it is based on V-I scan and on analysis of characteristic curve.

If we look at the characteristic of the PV system in a possible shadow condition, as reported in Figure 3.3, we observe the curve changes its convexity, so it can present one or more flexpoints. Researching these flexpoints (signed as P in figure), it will be possible to estimate and monitor eventually partial shadow conditions.

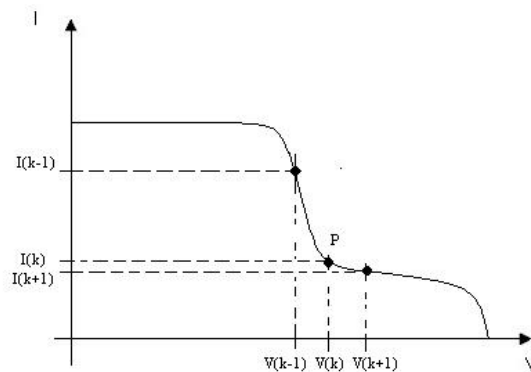


Figure 3.3. Generic V-I curve in partial shadow condition

Considering that it is possible to sample voltage signal and current signal in different time instant, the mathematical analysis will be based on numerical methods and in particular using the *finite-difference methods*: that is a numerical method to determinate numerical solutions of differential equations.

In the Appendix A, a short description of finite difference method is report [38, 39].

Let's introduce on voltage axes a partition so called $I_k=[k-1, k]$ with $k=2,3, \dots, N$. All these time partitions have the same length, on the contrary the intervals ΔV will not be all equal, depending $V(k)$ in that instant k :

$$\Delta V = V(k) - V(k-1) = V_k - V_{k-1} \quad (3.11)$$

Let's indicate then with $I(k)$ the sampled current to the correspondent voltage $V(k)$.

To study the convexity of the function and analyze a possible shadowing condition, we have to consider two equations that we report here in general form, the first in term of first derivative, the second in term of second derivative, in correspondence of point P, flexpoint.

$$\left. \frac{df}{dx} \right|_p < 0 \quad (3.12)$$

$$\left. \frac{d^2f}{dx^2} \right|_p > 0 \quad (3.13)$$

If the function $f(x)$ is smooth around P point, then the finite-different operator represent a good second derivative approximation and it can be written as:

$$\left. \frac{d^2f}{dx^2} \right|_p \simeq \frac{f(x_{k+1}) + f(x_{k-1}) - 2f(x_k)}{\Delta x^2} \quad (3.14)$$

Instead about first derivative, it will be necessary apply Euler's formula in the point x_k :

$$\left. \frac{df}{dx} \right|_p \simeq \frac{f(x_{k+1}) - f(x_k)}{\Delta x} \quad (3.15)$$

Let's report now these equations in our case applying conditions.

$$\left. \frac{d^2I}{dV^2} \right|_p \simeq \frac{I_{k+1} + I_{k-1} - 2I_k}{\Delta V^2} > 0 \quad (3.16)$$

$$\left. \frac{dI}{dV} \right|_p \simeq \frac{I_{k+1} - I_k}{\Delta V} < 0 \quad (3.17)$$

In the followed algorithm an important factor is the choice of the k points, because efficiency of algorithm will depend on them.

It is easy to think that the interval must be very small, but we have to consider two aspects:

- The first is that working with an electronic calculator some rounding off are considered, it means that V-I curve in a microscopic analysis can present some numerical variations or it could be due to noise signal of the system (an example of that is reported in Figures 3.6 and 3.7), this aspect will drive us to choice a large interval $[k-1, k]$ so avoid a wrong calculation, moreover the choice of a small sample interval will influence the calculation time.
- The second aspect is that if interval is very large, it could overcome the interest point and not find it. It's important to evidence that the worst case is when the algorithm finds a strong numerical variation in the sample interval, supplying a wrong result.

The choice of $[k-1, k]$ is, in this way, a compromise between precision and calculation speed.

In the graphs below, with '*' are shown the extremities of interval ΔV where partial shadow condition has been researched. These behaviors, with their work conditions, will be show in the next section, where results achieved by simulations of plant and reference model are reported.

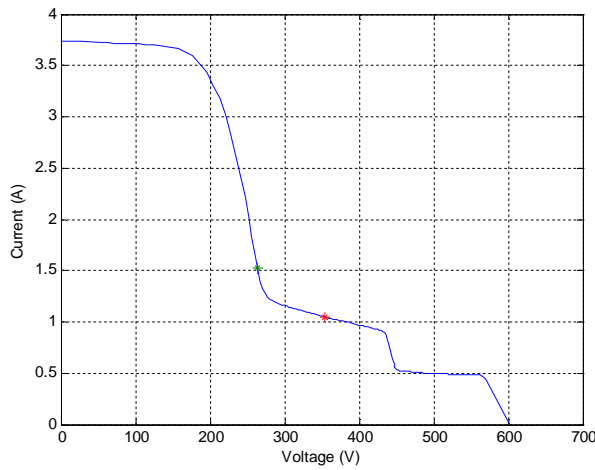


Figure 3.4. Detection partial shadow condition on V-I curve
 $G=959.6W/m^2$ $T=318.7K$

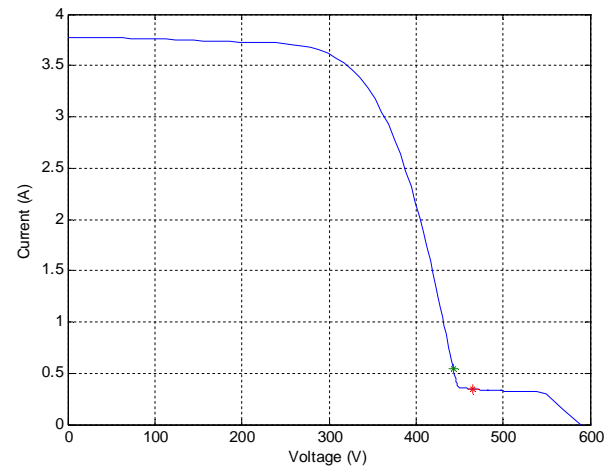


Figure 3.5. Detection partial shadow condition on V-I curve
 $G=963.4W/m^2$ $T=320.1K$

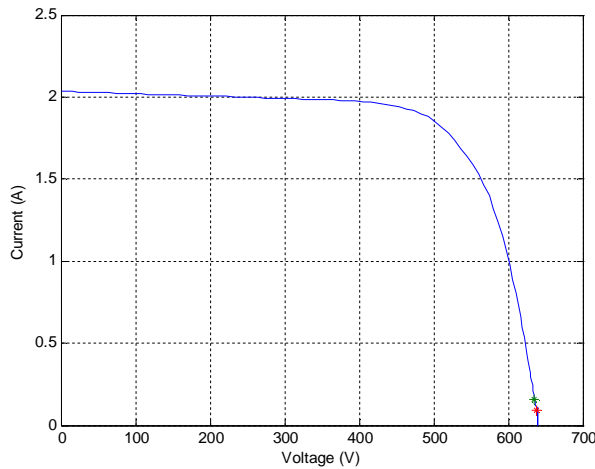


Figure 3.6. Error detection on V-I curve caused by a numerical variation (Figure 3.7) on a PV in normal condition

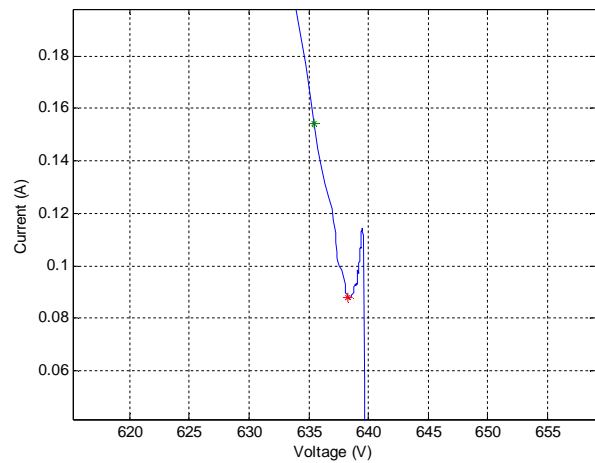


Figure 3.7. Error detection caused by a numerical variation on V-I curve

The error between PV current and the reference current further is an important aspect because it could influence the preview result, like in the case of a small partial shadow condition, the algorithm would not be able to find any shadow condition, anyway this error is very small and well accepted (an example is shown in Figure 3.8).

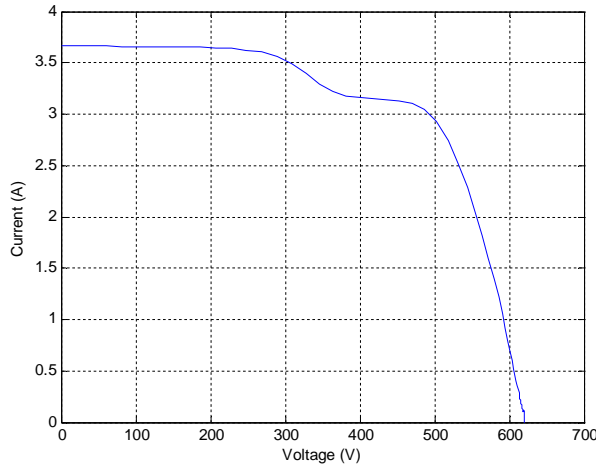


Figure 3.8 No detection of partial shadow condition on V-I curve caused by a small current error

In the project the sample interval $[k-1, k]$ and the error threshold ε have been chosen respectively:

$$[k-1, k] = 30 \text{ samples}$$

$$\varepsilon = 0.4 \text{ A}$$

The choice of sample interval has been based testing some sample lengths in both normal and shadowing condition. Considering an interval very short on plant in normal condition (for example 5 samples in a test of ours), the algorithm indicated a variation on the curve that has signaled like shadow condition, but it was caused by a numerical variation in the V-I curve, a small numerical variation detected by algorithm. Considering, instead, very large sample ranges on plant in shadowing condition (for example 60 samples in a test of ours), the algorithm overcame the point of interest. In this way our choice has been focus in a intermediate range avoiding any variation and detecting the real partial shadow condition. Considering 30 samples the results obtained have been acceptable.

A strong limitation, is the consideration of a smooth V-I curve, without strong numerical variations. This aspect is connected with first and second order derivatives.

The choice of the predictive error has been valued in the same moment, avoiding algorithm can be executed with an error too small. A small predictive error is good accepted.

3.3.2 PV PLANT CHARACTERISTICS AND SIMULATIONS

The PV plant that we have considered is composed by 16 photovoltaic panels: 120 Watt multicrystalline photovoltaic module. The MSX 120 is used primarily in large battery-equipped PV systems or, through an inverter, to provide AC power directly to a load, as reported on documentation [40].

Let's start reporting here, the electrical characteristics as on datasheets, these dates are calculated in STC condition.

	MSX 120	MSX 110 ⁴
Maximum power (P_{max}) ²	120W	110W
Voltage at P_{max} (V_{mp})	33.7V	33.6V
Current at P_{max} (I_{mp})	3.56A	3.3A
Minimum P_{max}	114W	105W
Short-circuit current (I_{sc})	3.87A	3.6A
Open-circuit voltage (V_{oc})	42.1V	41.6V
Temperature coefficient of I_{sc}	$(0.065 \pm 0.015)\%/^{\circ}C$	
Temperature coefficient of V_{oc}	$-(80 \pm 10)mV/^{\circ}C$	
Temperature coefficient of power	$-(0.5 \pm 0.05)\%/^{\circ}C$	
NOCT ³	$47 \pm 2^{\circ}C$	
Maximum system voltage	600V (U.S. NEC rating) 1000V (TÜV Rheinland rating)	
Maximum series fuse rating	20A	

Figure 3.9. MSX120 photovoltaic panel datasheets

Instead in Figure 3.10 the MSX 120 curves are shown.

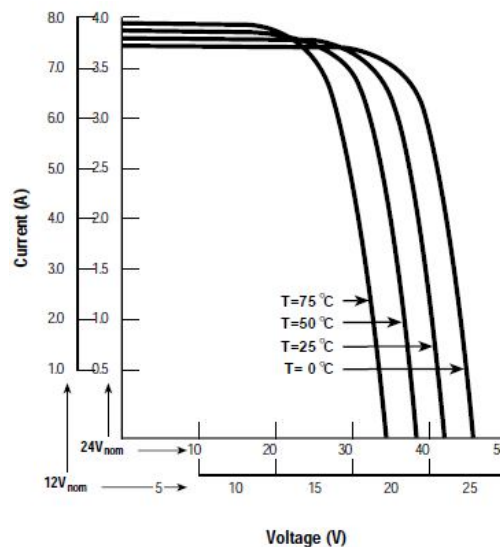


Figure 3.10. MSX120 VI curve

The PV system has been subjected to different irradiance levels, in nominal and shadowing condition.

The first three measures have been done in nominal conditions and here we report results obtained by simulation, for three different irradiation levels are applied: high, medium, low.

- High irradiance in the range $[1000 - 800] \text{ W/m}^2$: $G = 952.2 \text{ W/m}^2$, $T = 313.2 \text{ K}$

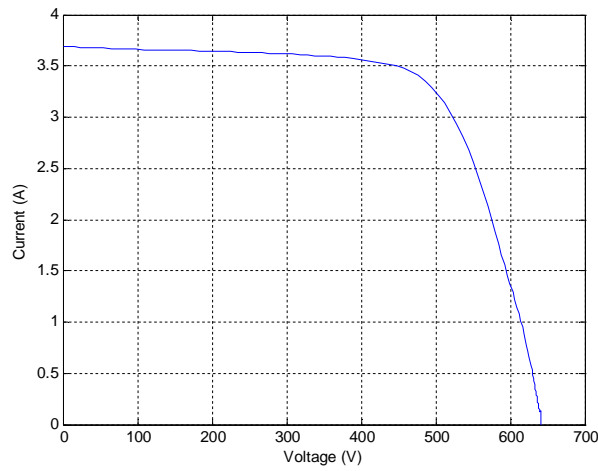


Figure 3.11. Measured plant V-I curve – High irradiance

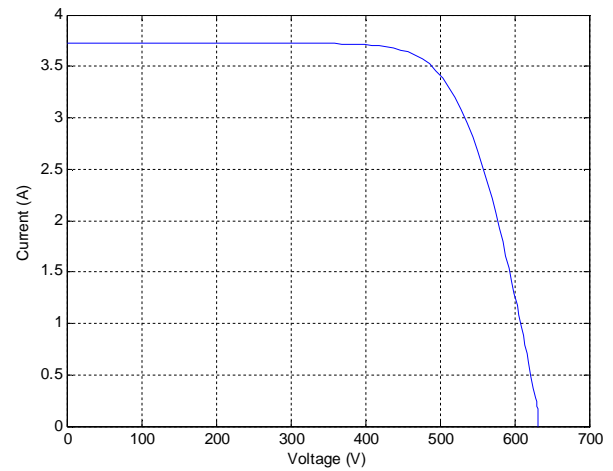


Figure 3.12. Reference V-I curve – High irradiance

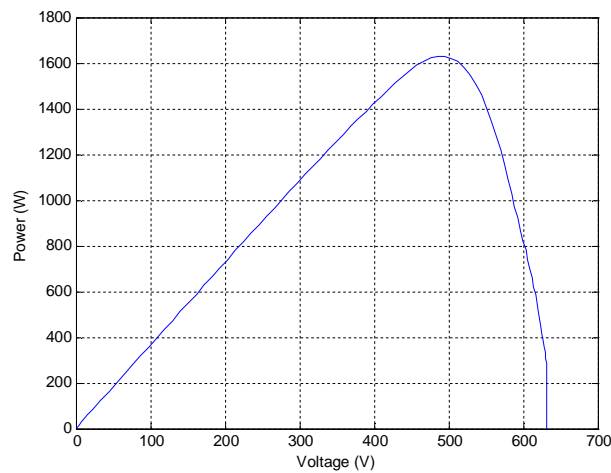


Figure 3.13. Power-voltage curve – High irradiance

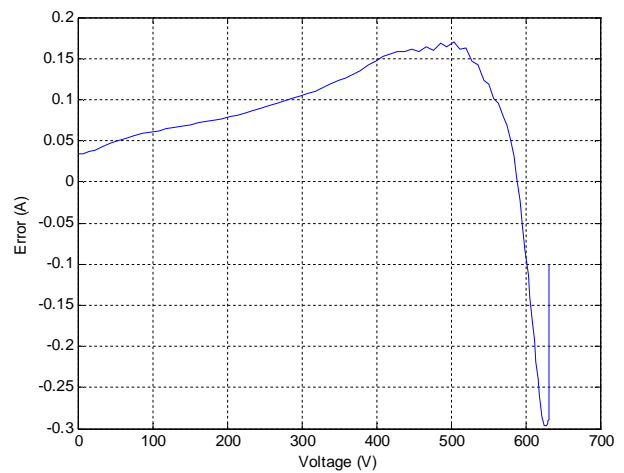


Figure 3.14. Predictive error – High irradiance

- Medium irradiance in the range [800-600] W/m²: $G=673.0$ W/m² , $T=315,8$ K

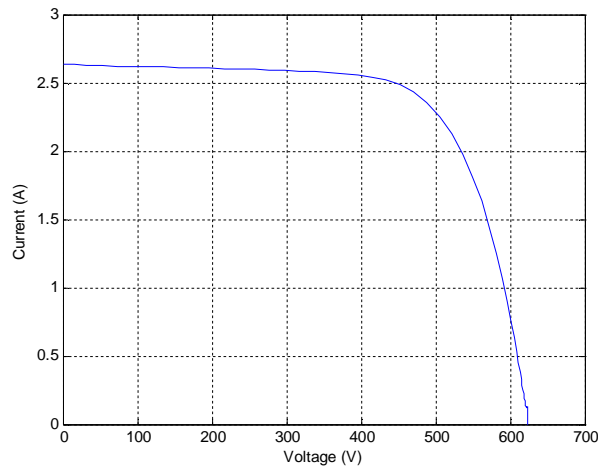


Figure 3.15. Measured plant V-I curve – Medium irradiance

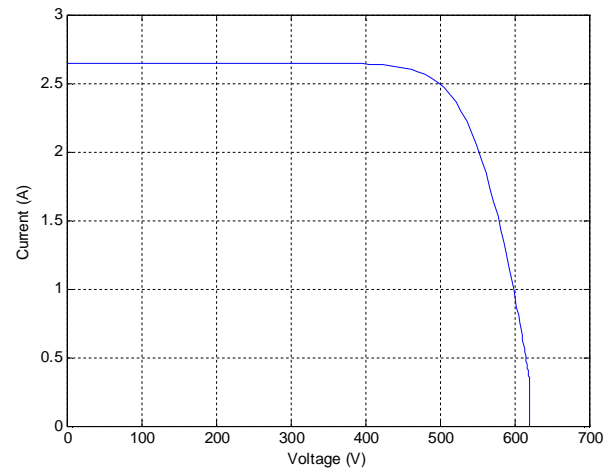


Figure 3.16. Reference V-I curve – Medium irradiance

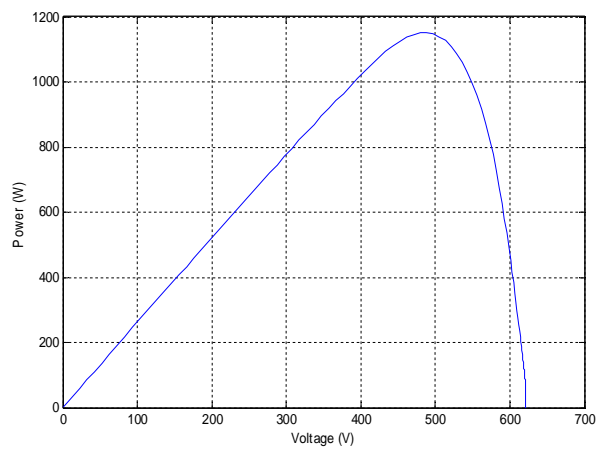


Figure 3.17. Power-voltage curve – Medium irradiance

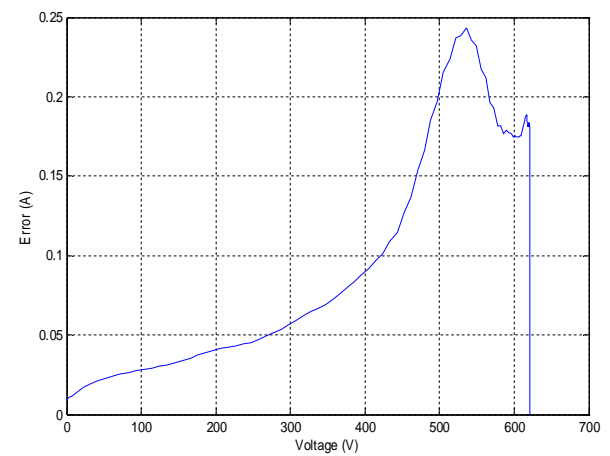


Figure 3.18. Predictive error – Medium irradiance

- Low irradiance in the range [600-400] W/m² : $G=503.6 \text{ W/m}^2$, $T= 303.8\text{K}$

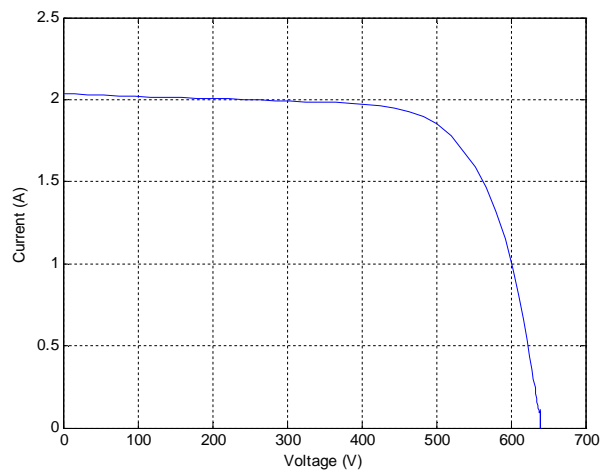


Figure 3.19. Measured plant V-I curve – Low irradiance

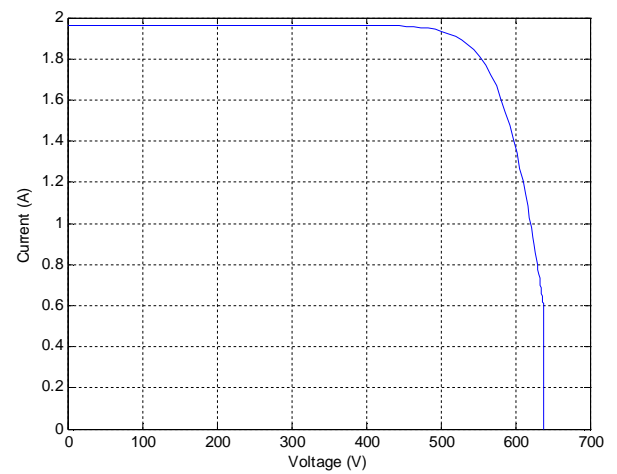


Figure 3.20. Reference V-I curve – Low irradiance

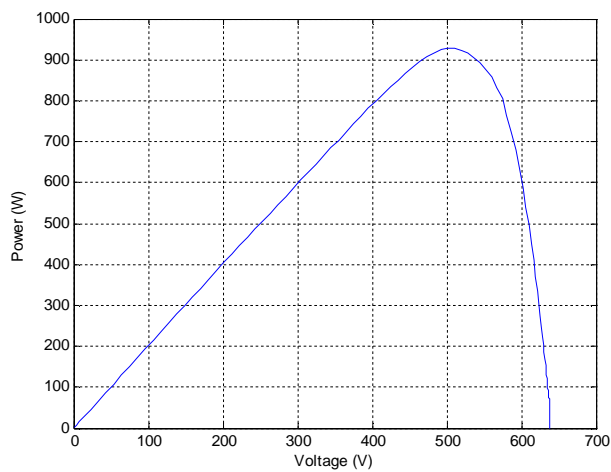


Figure 3.21. Power-voltage curve – Low irradiance

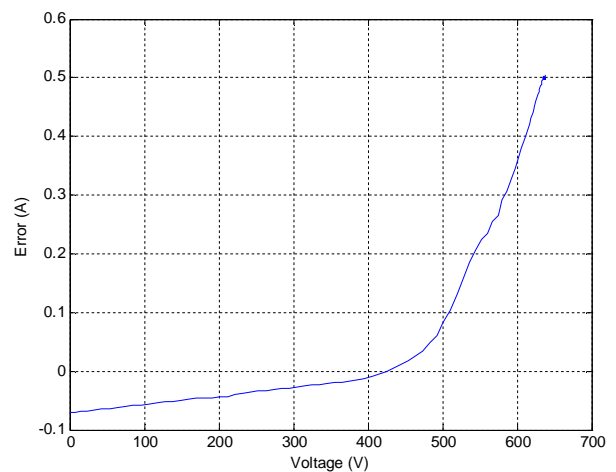


Figure 3.22. Predictive error – Low irradiance

Other measures have been done in partial shadow conditions:

- Partial shadow condition 1: $G=959.6 \text{ W/m}^2$, $T=318.7 \text{ K}$

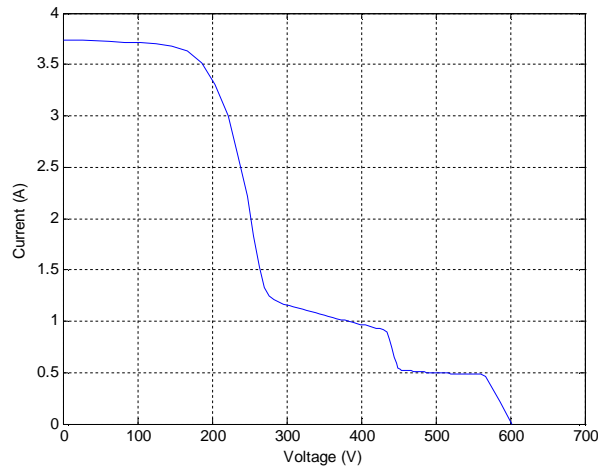


Figure 3.23. Measured plant V-I curve – Partial shadow condition 1

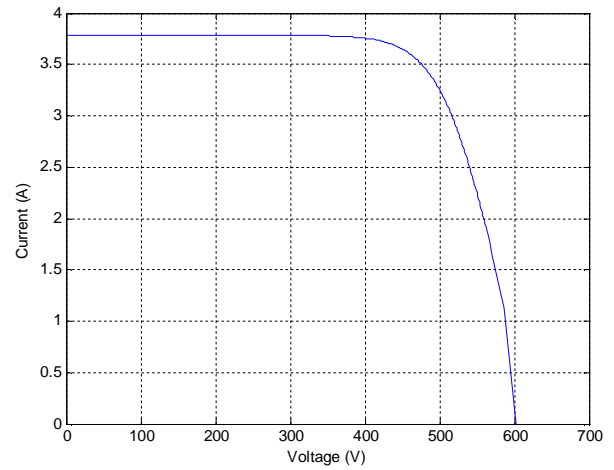


Figure 3.24. Reference V-I curve – Partial shadow condition 1

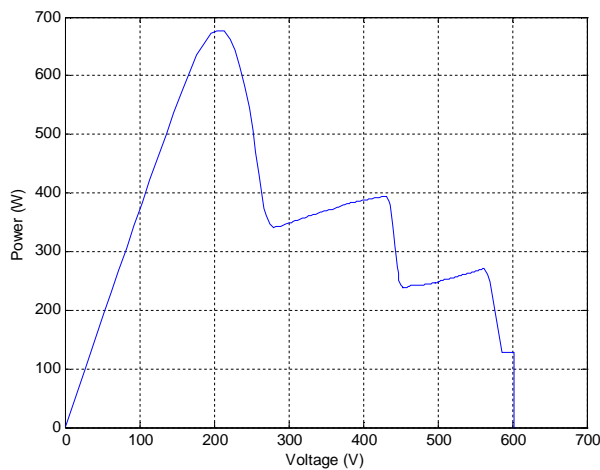


Figure 3.25. Power-voltage curve – Partial shadow condition 1

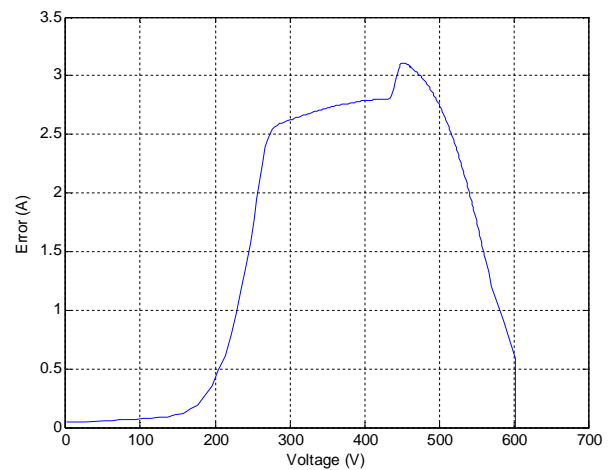


Figure 3.26. Predictive error – Partial shadow condition 1

- Partial shadow condition 2: $G=963.4 \text{ W/m}^2$, $T=320.1 \text{ K}$

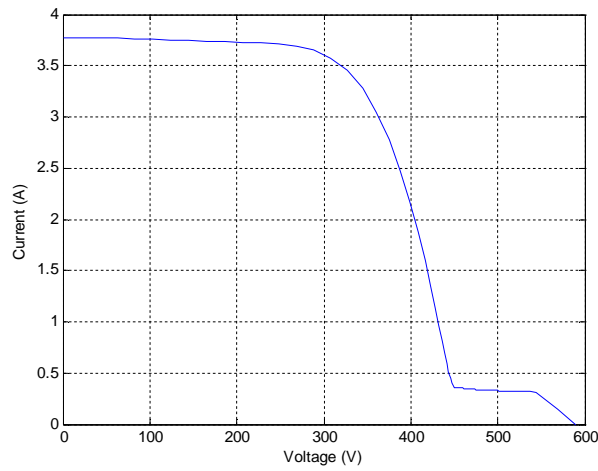


Figure 3.27. Measured plant V-I curve – Partial shadow condition 2

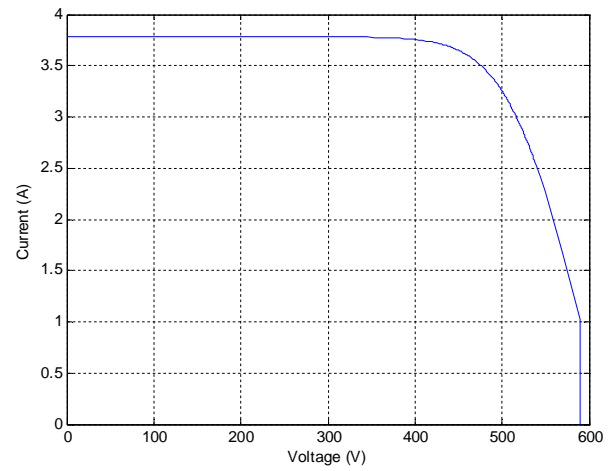


Figure 3.28. Reference V-I curve – Partial shadow condition 2

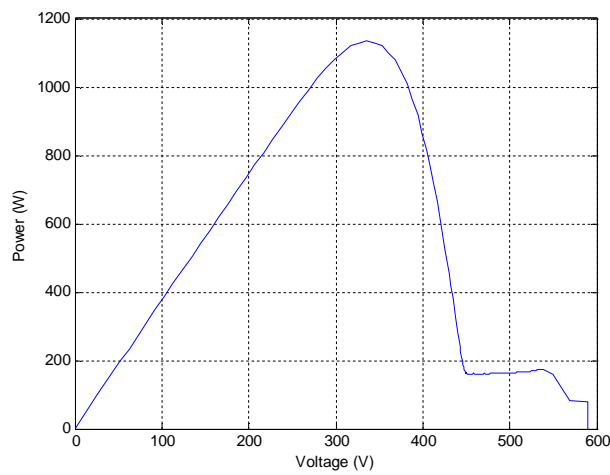


Figure 3.29. Power-voltage curve – Partial shadow condition 2

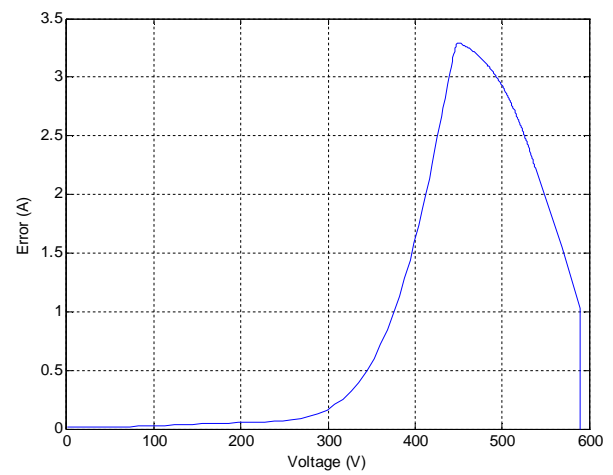


Figure 3.30. Predictive error – Partial shadow condition 2

- Partial shadow condition 3: $G=933 \text{ W/m}^2$, $T=320.51 \text{ K}$

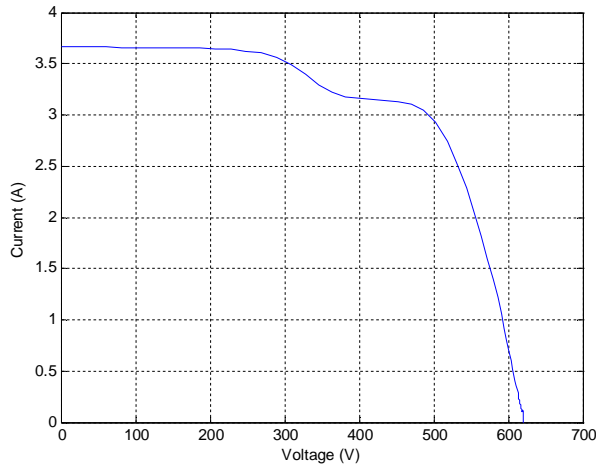


Figure 3.31. Measured plant V-I curve – Partial shadow condition 3

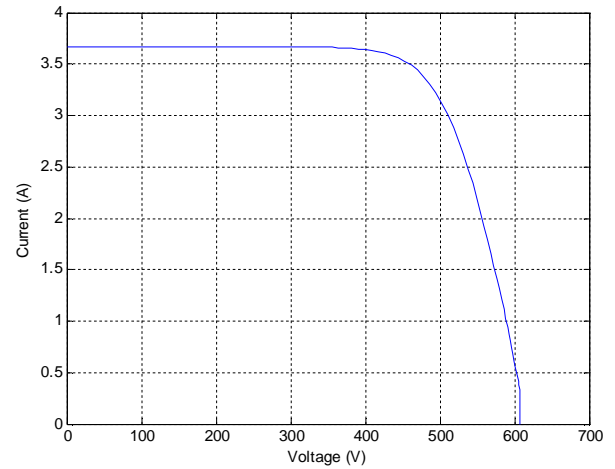


Figure 3.32. Reference V-I curve – Partial shadow condition 3

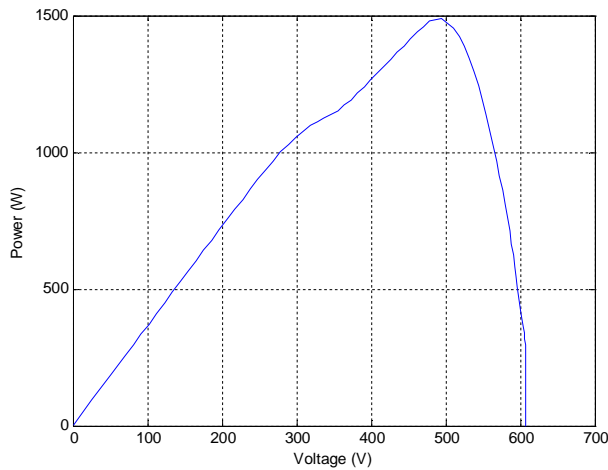


Figure 3.33. Power-voltage curve – Partial shadow condition 3

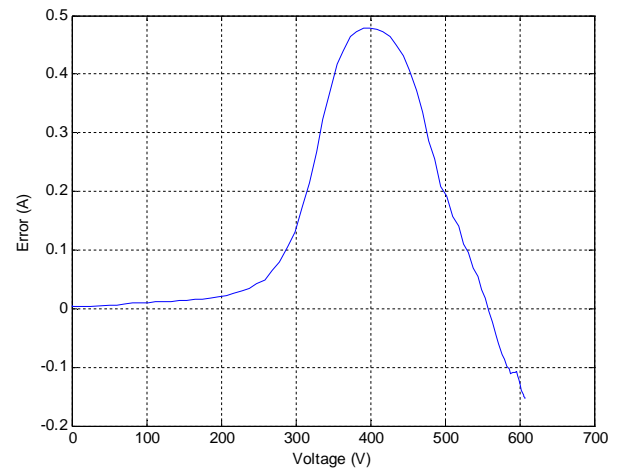


Figure 3.34. Predictive error – Partial shadow condition 3

A message has been displayed when algorithm detected a shadow condition.



Figure 3.35. Message of shadowing condition

For each one of them, 101 values of voltage and current has been sampled on the plant and 201 values are determinate for interpolation, considering then 16 panels in series at the same voltage, the array voltage is obtained as reported in (2.7) with $N_s=16$, so to achieve the characteristic curves of PV system.

3.3.3 ADJUSTMENT PARAMETERS MECHANISM

In this paragraph we want to test a mechanism to adjust the PV reference model parameters. As explained in last section, supervision control determines if the PV reference current is enough far from the real PV current, so that if the error is enough big, supervision control commands the estimator block to adjust the reference model parameters such that error could converge to the desired.

The mechanism here tested is based on *the Newton-Raphson method*, a numerical method for determination of the numerical solutions of non linear equations which solution is obtained as limit of a succession.

In the Appendix B, a short description of Newton-Raphson method is reported with its proof [39, 41].

Let's consider here a general nonlinear system equations:

$$\begin{cases} f_1(x_1, x_2, x_3, \dots, x_n) = 0 \\ f_2(x_1, x_2, x_3, \dots, x_n) = 0 \\ \vdots \\ f_n(x_1, x_2, x_3, \dots, x_n) = 0 \end{cases} \quad (3.18)$$

As described in Appendix B, this problem can be formulated as a limit of a succession:

$$-f(x^{(k)}) \cong J_f(x^{(k)})(x^{(k+1)} - x^{(k)}) \quad (3.19)$$

At each step, the mechanism has to resolve a linear system in the variable $(x^{(k+1)} - x^{(k)})$, for this the computational time is very high, however the loop can be stopped considering a stop criterion.

$$x^{k+1} \cong x^{(k)} - J_f^{-1}(x^{(k)})f(x^{(k)}) \quad (3.20)$$

This is the Newton-Raphson method, for a nonlinear system equations.

Let's try now, to apply this method to our system, and to test if we obtain a solution.

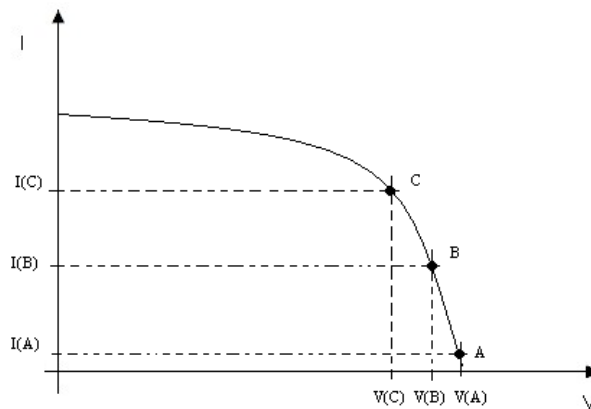


Figure 3.36. Newton-Raphson method applied to PV system

The idea is to consider a nonlinear system with three equations in three parameters unknown: I_o , V_t , R_s . We didn't consider I_{ph} , because from (3.7) is already known.

To obtain that system, we need three equations, achieved considering on the V-I curve just three points: A,B,C (shown in Figure 3.36) and consider the PV non linear equation (2.1) in respective points.

$$\begin{cases} I_A = I_{ph} - I_o \left(e^{\frac{V_A + I_A R_s}{V_t}} \right) \\ I_B = I_{ph} - I_o \left(e^{\frac{V_B + I_B R_s}{V_t}} \right) \\ I_C = I_{ph} - I_o \left(e^{\frac{V_C + I_C R_s}{V_t}} \right) \end{cases} \quad (3.21)$$

If we value the equation (2.1) in V_A , V_B and V_C , the non linear system (3.18) becomes as in (3.22)

$$\begin{cases} I_A - I_{ph} + I_o \left(e^{\frac{V_A + I_A R_s}{V_t}} \right) = 0 \\ I_B - I_{ph} + I_o \left(e^{\frac{V_B + I_B R_s}{V_t}} \right) = 0 \\ I_C - I_{ph} + I_o \left(e^{\frac{V_C + I_C R_s}{V_t}} \right) = 0 \end{cases} \quad (3.22)$$

To determinate step by step the algorithm (3.20) we need to determinate the Jacobian matrix in the parameters vector (I_o , V_t , R_s), matrix here calculated

$$J = \begin{pmatrix} -1 + \left(e^{\frac{V_A + I_A R_s}{V_t}} \right) & -I_o e^{\frac{V_A + I_A R_s}{V_t}} \left(\frac{V_A + I_A R_s}{V_t^2} \right) & I_o e^{\frac{V_A + I_A R_s}{V_t}} \left(\frac{I_A}{V_t} \right) \\ -1 + \left(e^{\frac{V_B + I_B R_s}{V_t}} \right) & -I_o e^{\frac{V_B + I_B R_s}{V_t}} \left(\frac{V_B + I_B R_s}{V_t^2} \right) & I_o e^{\frac{V_B + I_B R_s}{V_t}} \left(\frac{I_B}{V_t} \right) \\ -1 + \left(e^{\frac{V_C + I_C R_s}{V_t}} \right) & -I_o e^{\frac{V_C + I_C R_s}{V_t}} \left(\frac{V_C + I_C R_s}{V_t^2} \right) & I_o e^{\frac{V_C + I_C R_s}{V_t}} \left(\frac{I_C}{V_t} \right) \end{pmatrix} \quad (3.23)$$

We want to present now, an algorithm which has been run to determinate the three parameters of interest. It is shown in Figure 3.37.

In the first step, initial values are assigned from parameters estimation system (3.7), a tolerance is necessary to stop the algorithm if the error, between the parameters vector in the time k and the same parameters vector in the time $k-1$, is greater than it, expressed with TOLL.

The algorithm stops also if the iteration numbers is greater than NMAX, maximum number of iterations, at each loop it increase by one.

The algorithm Newton-Raphson at each iterations determinates the system (3.22) and Jacobian matrix as in (3.23) to determinate then the parameters vector in the step (k+1) as reported in the equation (3.20)

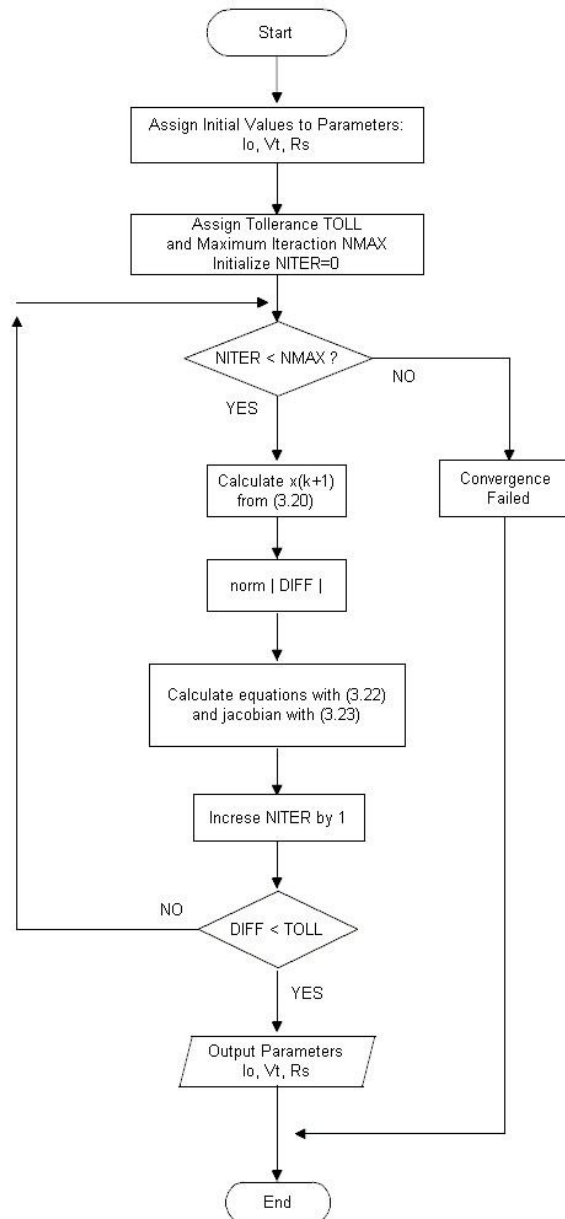


Figure 3.37. Newton-Raphson algorithm to determinate parameters of PV system

In this project the algorithm presented above, has been applied many times on PV model in normal condition, so that, if the error is greater than threshold value but the supervision control doesn't detect any partial shadow condition, this algorithm is run.

The algorithm has been applied in low irradiance (the only one case in normal condition to have error greater than threshold) but every time, MatLab has presented the same result: Convergence Failed. The experiment has been applied also increasing the tolerance and iteration number, but results we obtained leave to think that Jacobian matrix converges being singular, that means multiple solutions can exist.

4 CONCLUSION

In this project we had wanted to realize an advanced control applied to a photovoltaic system to monitor the work conditions, in normal or in shadowing weather conditions.

Measuring voltage signal and current signal on PV panel, considering that the array of interest is composed by sixteen panels in series, a model of plant has been realized interpolating dates and determining respectively the output voltage and current in correspondence of the max power point.

The supervision control we have realized is based on MRAS system: Model Reference Adaptive System, so to estimate and predictive the PV system behavior, a behavior based on a non linear mathematical model, and step by step it executes an algorithm control, on the hand to monitor the real PV system conditions, on the other hand it should correct parameters of reference model.

The difference between the predictive response and the real response of the system is called *prediction error*, the monitoring algorithm control can analyze and establish if PV system is working in normal or shadow condition.

In the first step, the model is entirely based on the datasheet parameters given by the manufacturer, and experimental results showed model is accurate, that is the error is smaller than a threshold value.

If the prediction error overcomes the threshold, the monitoring algorithm scans the V-I curve, researching a possible shadow condition, analyzing the first and second order derivatives.

The algorithm presented here, works very well if V-I curve is enough smooth and strong current variations are off, but anyway the choice of sample time and numerical errors can influence the results.

As we said, an advanced and predictive control must be able also to correct its parameters in automatically way, so to have a good estimation of real behavior and satisfy the objective function, that is to minimize the predictive error, but here we wanted just to test a strategy based on Newton-Raphson method. The result we achieved by simulation has been negative, but it can be improved, improving the model and the algorithm.

With this project we had wanted to put the basic to realize more complex advanced system control based on MRAS that be able to maximize the efficient of a PV system, predicting and researching in the minor time the maximum power point (MPP).

All results have been achieved modeling all systems in Simulink and writing all models in MatLab code. The schemes which we focused on, include the PV plant model, the parameters estimator, the reference model block and the supervision system control.

The MPPT block, necessary to track the maximum power point and establish to reference voltage in input, is based on the algorithm Perturb and Observe, which, step by step researches the point which for the first order derivative is zero.

About, conversion system, a single stage converter DC/AC has been used and on it a voltage and current control has been used to apply on grid the voltage and current required.

The project presented here, can be a first step which on a lot of research can be still done, trying to improve or to find new parameter estimation laws, and also to improve the reference model of PV plant, considering a model with five or more parameters so to satisfy better the object function proposed here.

Concluding, nowadays photovoltaic energy field is increasing and to reduce energy costs and reduce the use of traditional energy source, we have to focus on it investigating and researching new technologies, new solutions.

APPENDICES

A. FINITE DIFFERENCE METHOD

In this appendix we will discuss about numerical solution of differential equations using the *finite different method*, this theory is applicable also to partial differential equations, but here we will deal with mono-dimensional problem. So the problem is how to approximate the differential operator in the most easy way as possible.

The finite difference method to determinate a solution of a problem with outline conditions, is applied in two steps:

1. To substitute at smooth domain Ω a discrete domain composed by a finite number of points, including the border $\partial\Omega$.
2. To approximate on the discrete domain all derivatives and the condition on border.

In that way a smooth continue mathematic problem is approximate to a discrete problem with a finite number of easier equations in a finite number.

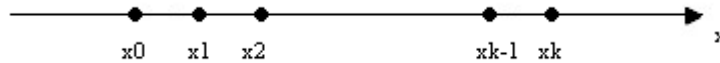
Let's apply the finite difference method to solve the following problem: determinate $u=u(x)$ in the range $[0, l]$ such that so satisfy the equation:

$$\frac{d^2 u(x)}{dx^2} = f(x) \quad (A.1)$$

with $x \in [0, l]$ and condition on the border, the following conditions are called *Dirichlet conditions*.

$$\begin{cases} u(0)=x_0 \\ u(l)=x_1 \end{cases} \quad (A.2)$$

if the function $f(x)$ is limited in $(0, l)$, the solutions and its first derivative are smooth in the range.



Let 's introduce on the range $[0, l]$ now a partition $I_k=[x_{k-1}, x_k]$ with $k=1, 2, \dots, N, N+1$, with $x_0=0$ and $x_{N+1}=l$, as in Figure, let's assume that intervals have all the same length $\Delta x=x_k-x_{k-1}$:

$$\Delta x = \frac{l}{N+1} \quad (A.3)$$

and with $u(x_k)$ $k=0, 1, \dots, N, N+1$ the sampled function values in the point of the grid. Assuming that $f_k=f(x_k)$ in all points of the range, we obtain with $k=1, 2, \dots, N$

$$\left. \frac{d^2 u}{dx^2} \right|_{x=x_k} = f_k \quad (A.4)$$

If the function $u(x)$ is smooth around the point x_k the finite difference operation can be written as:

$$\delta^2 u(x_k) = \frac{u(x_k + \Delta x) - 2u(x_k) + u(x_k - \Delta x)}{\Delta x} \quad (A.5)$$

(A.5) represents a good approximation of the second derivative:

$$\left. \frac{du}{dt} \right|_{t=t_k} \cong \frac{u_{k+1} - u_k}{\Delta t} \quad \left. \frac{d^2 u}{dx^2} \right|_{x=x_k} = \frac{u(x_k + \Delta x) - 2u(x_k) + u(x_k - \Delta x)}{\Delta x} + o(\Delta x) \quad (A.6)$$

$$\left. \frac{d^2 u}{dx^2} \right|_{x=x_k} \cong \delta^2 u(x_k) = \frac{u(x_k + \Delta x) - 2u(x_k) + u(x_k - \Delta x)}{\Delta x} \quad (A.7)$$

In that way we obtain the system of N equations, with $k=1, 2, \dots, N$

$$\frac{u(x_{k+1}) - 2u(x_k) + u(x_{k-1}))}{\Delta x} = f_k \quad (A.8)$$

This is the approximation of equation (A.4) achieved approximating the second derivative operation with finite difference operation.

This operation is said *consistent*, it means that for $\Delta x \rightarrow 0$ the finite difference operation converges to derivative.

The system of equations can be used to re-write an algebraic linear system equations in uncertainties u_1, u_2, \dots, u_N , but here we will not report any proof on it, just we had wanted to introduce the approximation of the derivative operation.

It's important to evidence that every time we solve a problem using the finite difference method, we use a calculator, so we have to consider some rounding off errors, that can influence the solution.

Now we want to deal with first derivative, using finite derivatives method, here we will not consider the problem of Cauchy, which is a more generic problem, but we will focus on Euler's formula.

Let's begin considering the first derivative of a generic function $u(x)$ in a range $[t_0, t_f]$, and $f(u, t)$ a known function

$$\frac{du}{dt} = f(u, t) \quad (A.9)$$

and let's consider a partition of integration range $I=[t_0, t_f]$ in N sub-intervals $I_k=[t_{k-1}, t_k]$ of finite length with discrete step Δx :

$$\Delta t = \frac{t_f - t_0}{N} \quad (A.10)$$

We want to determinate the uncertainties functions $u(t)$ in the different points time $t_1, t_2 \dots t_k \dots$, and considering that for $\Delta t \rightarrow 0$ the number of intervals converge to infinity, the solution converges to $u(t)$, but working on an electronic computer it's evident to consider $\Delta t \neq 0$ but very short. If $u(t)$ is smooth, it can develop with second order Taylor's formula around t_k :

$$u_{k+1} = u_k + \left. \frac{du}{dt} \right|_{t=t_k} \Delta t + \frac{1}{2} \left. \frac{d^2u}{dt^2} \right|_{t=t_k} \Delta t^2 \quad (\text{A.11})$$

From (A.11) we can have:

$$\left. \frac{du}{dt} \right|_{t=t_k} = \frac{u_{k+1} - u_k}{\Delta t} - \frac{1}{2} \left. \frac{d^2u}{dt^2} \right|_{t=t_k} \Delta t \quad (\text{A.12})$$

And for $\Delta t \rightarrow 0$ the second term on the right converges to zero, while the first term converges a finite value, generally different then zero, that result is useful to approximate the first derivative of u in t_k with the finite difference

$$\left. \frac{du}{dt} \right|_{t=t_k} \cong \frac{u_{k+1} - u_k}{\Delta t} \quad (\text{A.13})$$

The formula (A.13) is called: the Euler's Formula, and the error we have in a the approximation is very small so to be well accepted [38, 39].

B. NEWTON-RAPHSON METHOD

In this appendix we will discuss about the determination of solution of a nonlinear system equations. We will deal with the nonlinear problem in the form written in (B3), let's consider then a vector function $\mathbf{f}(\mathbf{x})$ with \mathbf{x} uncertainties vector in domain $\mathbb{R}^n \supseteq D$ and image $\mathbb{R}^n \supseteq C$.

$$\mathbf{f}(\mathbf{x}) = [f_1(x_1, x_2, \dots, x_n), f_2(x_1, x_2, \dots, x_n), \dots, f_n(x_1, x_2, \dots, x_n)]^T \quad (\text{B.1})$$

$$\mathbf{x} = [x_1, x_2, \dots, x_n]^T \quad (\text{B.2})$$

We want to find the uncertainties vector \mathbf{x} such that:

$$\begin{cases} f_1(x_1, x_2, x_3, \dots, x_n) = 0 \\ f_2(x_1, x_2, x_3, \dots, x_n) = 0 \\ \vdots \\ f_n(x_1, x_2, x_3, \dots, x_n) = 0 \end{cases} \quad (\text{B.3})$$

That is a problem with n nonlinear equations in n uncertainties and the solution are called *zeros* of function \mathbf{f} .

A system expressed in (B3) can have just one solution, no solution or many solutions. For the system (B.3) the solution exists if:

1. The image space includes zero.
2. The function \mathbf{f} is an omeomorphism, that is the correspondence is one to one and the inverse is a continue function.

Generally methods most used to solve a nonlinear system equations, are iterative methods.

The solution is achieved as a limit of a succession.

Let's begin developing the function $\mathbf{f}(\mathbf{x})$ in Taylor series around $\mathbf{x}^{(k)}$ stopping to linear term.

$$f_i(\mathbf{x}) \cong f_i(\mathbf{x}^{(k)}) + \sum_{j=1}^n \left. \frac{\partial f_i}{\partial x_j} \right|_{\mathbf{x}=\mathbf{x}^{(k)}} (\mathbf{x}_j - \mathbf{x}_j^{(k)}) \quad (\text{B.4})$$

with $i=1,2,\dots,n$.

The n equations in (B.4) can be represented in vector form:

$$\mathbf{f}(\mathbf{x}) \cong \mathbf{f}(\mathbf{x}^{(k)}) + \mathbf{J}_f(\mathbf{x}^{(k)}) (\mathbf{x} - \mathbf{x}^{(k)}) \quad (\text{B.5})$$

where $\mathbf{J}_f(\mathbf{x}^{(k)})$ is the Jacobian matrix of function \mathbf{f} (B.1) valuated in parameter \mathbf{x} at step k .

The Newton-Raphson method is determinated:

$$-\mathbf{f}(\mathbf{x}^{(k)}) = \mathbf{J}_f(\mathbf{x}^{(k)}) (\mathbf{x}^{(k+1)} - \mathbf{x}^{(k)}) \quad (\text{B.6})$$

At each step, the mechanism has to resolve a linear system in the variable $(\mathbf{x}^{(k+1)} - \mathbf{x}^{(k)})$, for this the computational time is very high, however the loop can be stopped considering a stop criterion.

$$\mathbf{x}^{k+1} \cong \mathbf{x}^{(k)} - \mathbf{J}_f^{-1}(\mathbf{x}^{(k)}) \mathbf{f}(\mathbf{x}^{(k)}) \quad (\text{B.7})$$

This is the law of Newton-Raphson for a nonlinear system equations [39, 41].

C. SIMULINK® SCHEMES

In this paragraph we want to report all schemes used in Simulink® to realize the project presented.

In particular we focused on the plant, estimation parameters block, reference model and supervision control. All other blocks, realized by supervisor Dzeso Sera, have been used as support to realize the advanced control and monitoring system algorithm.

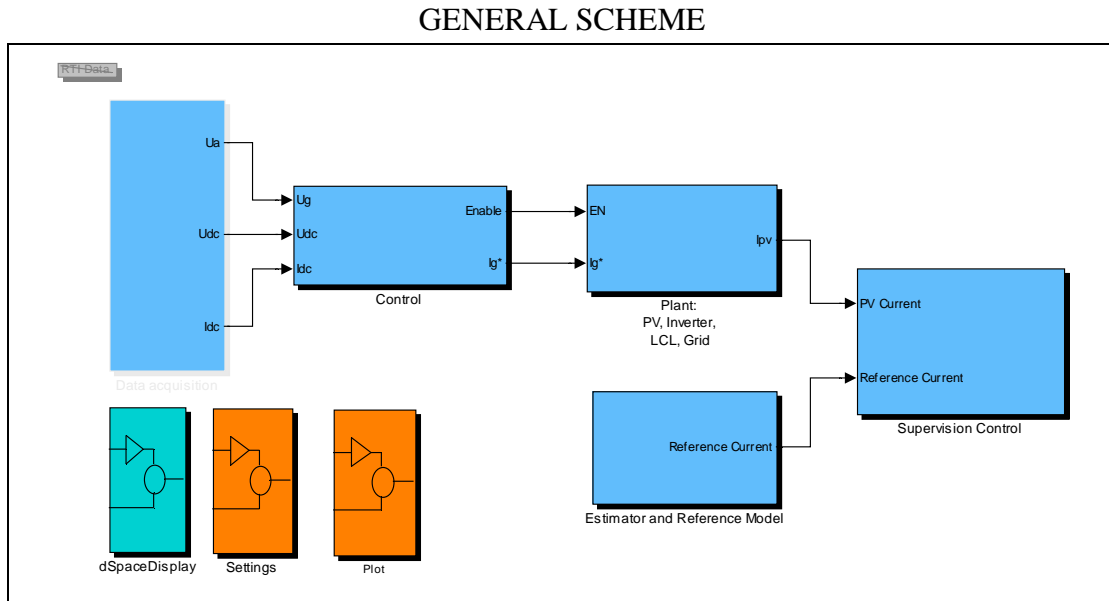


Figure C.1. General Scheme of PV system: Control, Data Acquisition, Inverter, LCL and Grid realized by Dzeso Sera

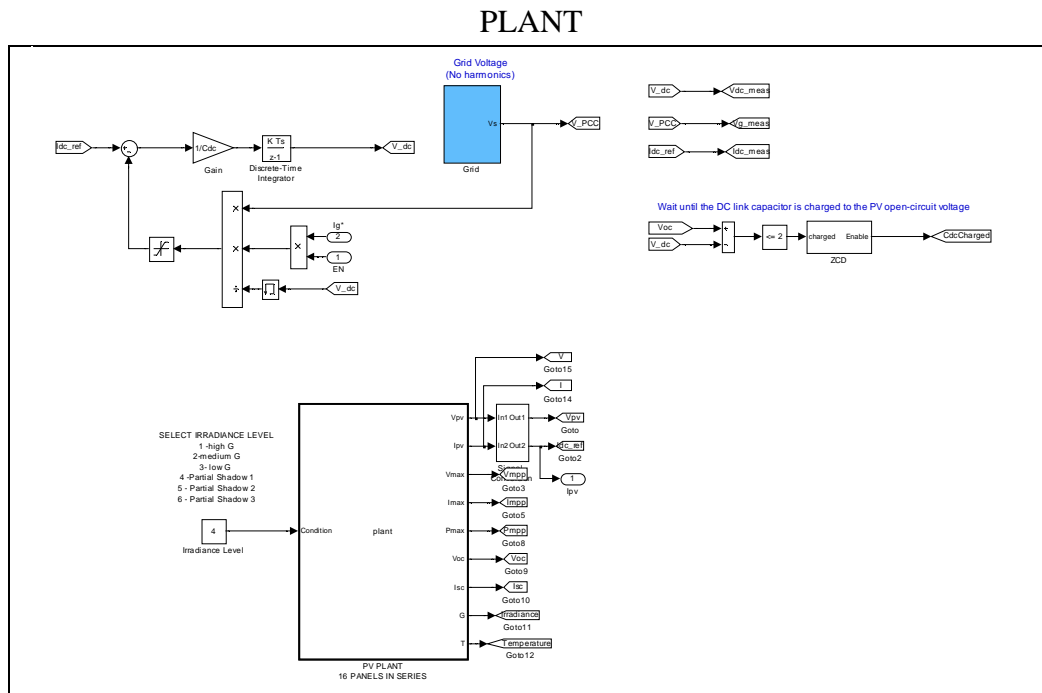


Figure C.2. Plant of PV system: Grid realized by Dzeso Sera

PARAMETERS ESTIMATOR and REFERENCE MODEL

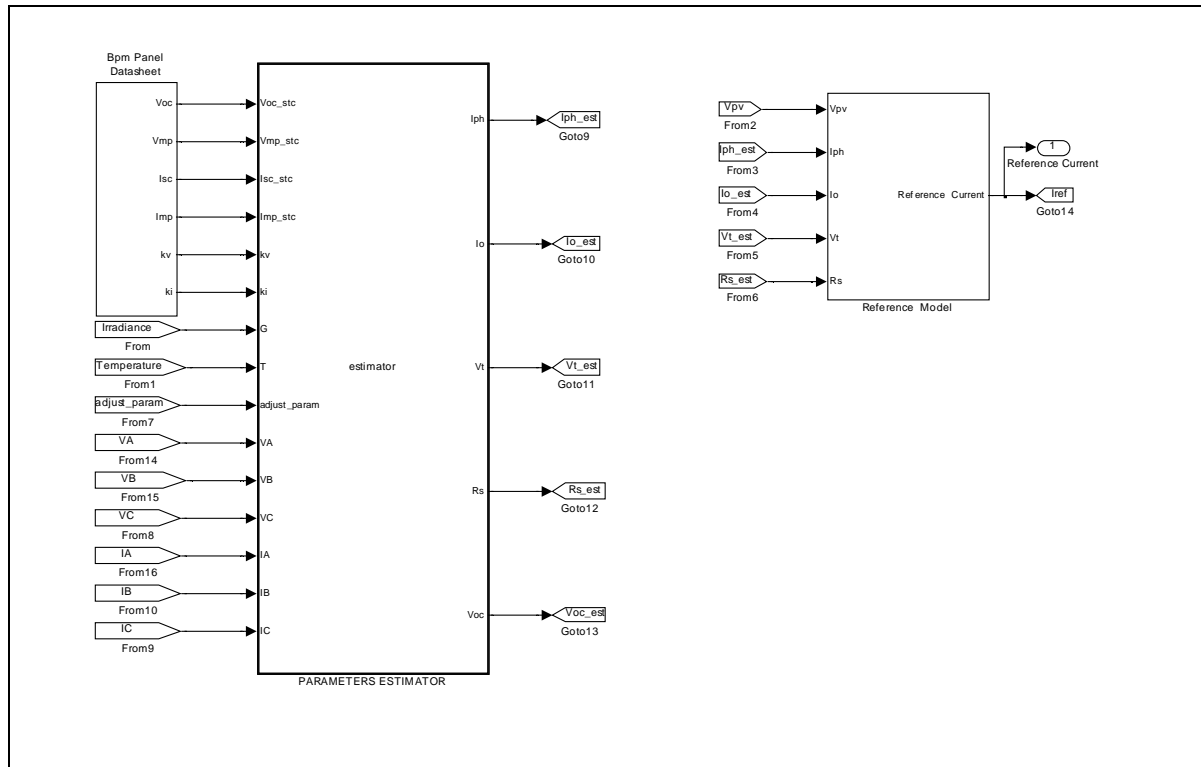


Figure C.3. Parameters estimator and reference model of PV system

SUPERVISION CONTROL

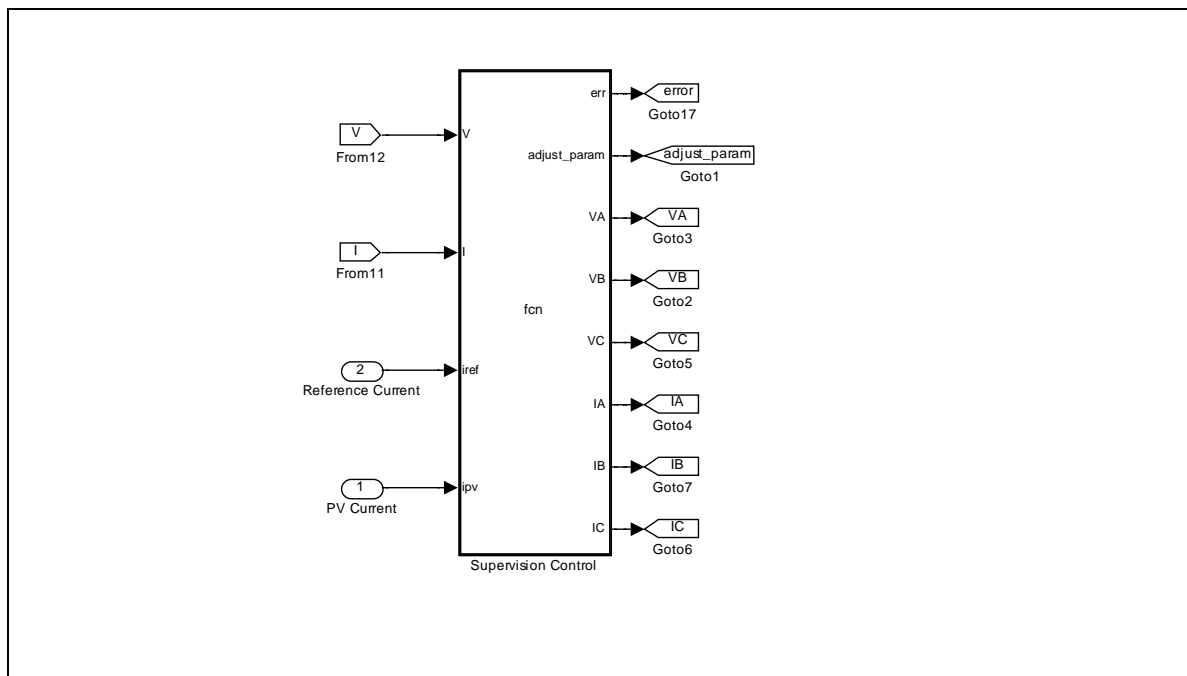
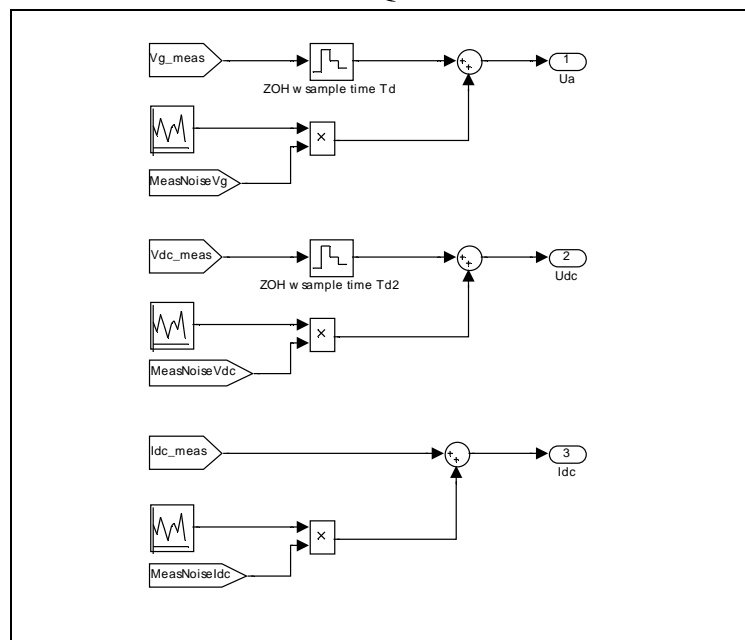
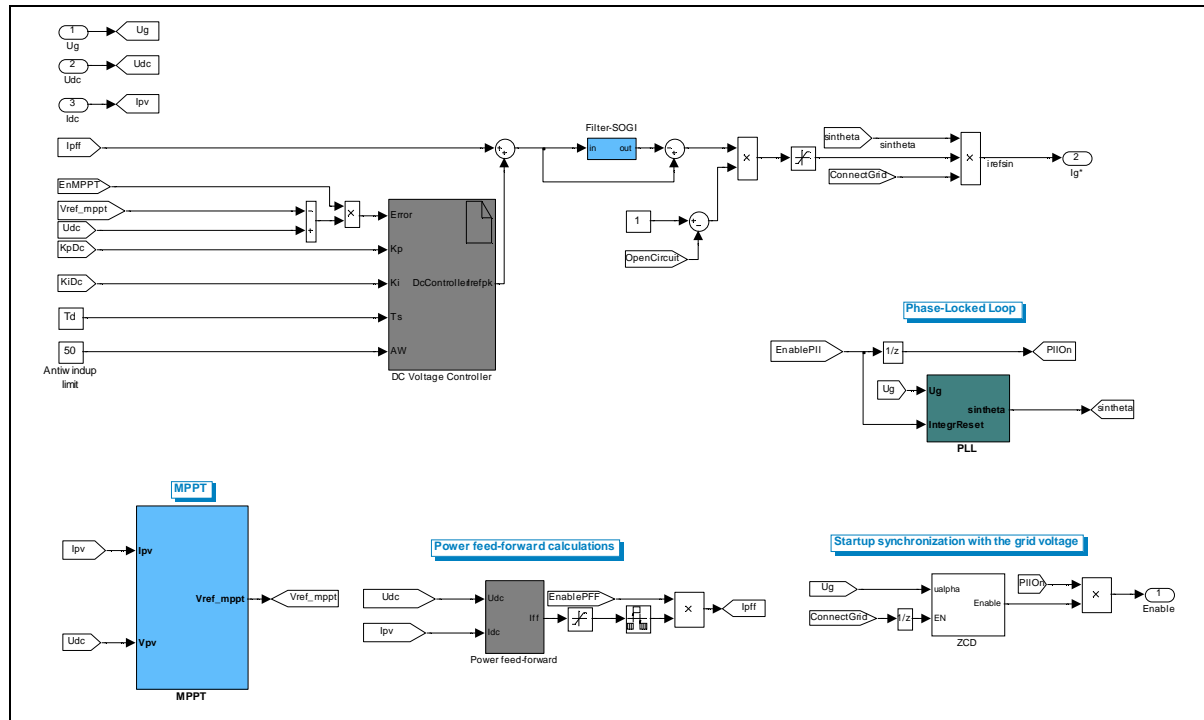


Figure C.4. Supervision control of PV system



D. MATLAB® CODE

In this paragraph all Matlab codes of Simulink blocks will be report, in the following order: Plant which block is shown in Figure C.2 , Estimator and Reference Model which block is in Figure C.3, Supervision Control which block is shown in Figure C.4

PLANT MATLAB CODE

```
function [Vpv,Ipv,Vmax,Imax,Pmax,Voc,Isc,G,T]=plant(Condition)
%eml DEFINITION FUNCTIONS
eml.extrinsic('xlsread');
eml.extrinsic('plot');
% PARAMETERS INITIALIZATION
V=zeros(1,101);
I=zeros(1,101);
Vpv=zeros(1,201);
Ipv=zeros(1,201);
Varray=0;
Iarray=0;
Pmax=0;
Imax=0;
Vmax=0;
G=0;
T=0;

% SELECTION PV CONDITION
switch Condition
case 1 % TEMP=313K IRRAD=952.2w/m^2 (G high level, 800-1000)
    V=xlsread('c:\Documents\MATLAB\tablevoltage.xls','table','A1:CW1');
    I=xlsread('c:\Documents\MATLAB\tablecurrent.xls','table','A1:CW1');
    G=952.2;
    T=313.2;
case 2 % TEMP=315K IRRAD=673.0w/m^2 (G medium, 600-800)
    V=xlsread('c:\Documents\MATLAB\tablevoltage.xls','table','A2:CW2');
    I=xlsread('c:\Documents\MATLAB\tablecurrent.xls','table','A2:CW2');
    G=673;
    T=315.8;
case 3 % TEMP=303.8K IRRAD=503.6w/m^2 (G low level, 400-600)
    V=xlsread('c:\Documents\MATLAB\tablevoltage.xls','table','A3:CW3');
    I=xlsread('c:\Documents\MATLAB\tablecurrent.xls','table','A3:CW3');
    G=503.6;
    T=303.8;
case 4 % TEMP=318.7K IRRAD=959.0w/m^2 Partial shadow
    V=xlsread('c:\Documents\MATLAB\tablevoltage.xls','table','A4:CW4');
    I=xlsread('c:\Documents\MATLAB\tablecurrent.xls','table','A4:CW4');
    G=959.6;
    T=318.7;
case 5 % TEMP=320.1K IRRAD=963.4w/m^2 Partial shadow
    V=xlsread('c:\Documents\MATLAB\tablevoltage.xls','table','A5:CW5');
    I=xlsread('c:\Documents\MATLAB\tablecurrent.xls','table','A5:CW5');
    G=963.4;
    T=320.1;
case 6 % TEMP=320.5K IRRAD=933w/m^2 Partial shadow
    V=xlsread('c:\Documents\MATLAB\tablevoltage.xls','table','A6:CW6');
    I=xlsread('c:\Documents\MATLAB\tablecurrent.xls','table','A6:CW6');
    G=933.0;
    T=320.5;
end

% INTERPOLATION V-I FOR SINGLE PANEL
Vpv(1)=V(1);
k=2; ii=1;
while k<201
```

```

Vpv(k)=(V(ii)+V(ii+1))/2;
k=k+1;
ii=ii+1;
Vpv(k)=V(ii);
k=k+1;
end
Ipv=interp1(V,I,Vpv);

% VOLTAGE CURRENT FOR ARRAY=16 PANELS
Varray=Vpv.*16;
Iarray=Ipv;

% DETERMINATION POWER CURVE
Parray=Varray.*Iarray;

% DETERMINATION Pmax Vmax Imax Isc Voc
[Pmax,position_max]=max(Parray)
Vmax=Varray(position_max);
Imax=Iarray(position_max)
Isc=Iarray(1);
Voc=Varray(length(Varray));

```

SUPERVISOR CONTROL

```

function [err,adjust_param,VA,VB,VC, IA,IB,IC]= fcn(V,I, iref, ipv)
eml.extrinsic('plot');
% INITIALIZATION INDEX DETECTION
i1=1;
i2=30;
i3=59;
PS=0; % PARTIAL SHADOW DETECTION VARIABLE

adjust_param=0; % ADJUSTMENT PARAMETERS SIGNAL
VA=V(length(V)-2);
VB=V(length(V)-20);
VC=V(length(V)-50);
IA=I(length(V)-2);
IB=I(length(V)-20);
IC=I(length(I)-50);

% MONITORING ALGORITHM CONTROL
err=iref-ipv;
if ((err>0.4)|| (err<-0.4))
    while (i3<=length(V)) && (PS==0)
        D2=(I(i3)+I(i1)-2*I(i2))/(V(i3)-V(i2))^2;
        D1=(I(i3)-I(i2))/(V(i3)-V(i2));
        if D2>0 && D1<0
            PS=1;
        else
            i1=i2;
            i2=i3;
            i3=i3+29;
        end
    end
    if PS==0
        adjust_param=1;
    end
end

if (i3<=length(V)) && PS==1
    V=V.*16;
    plot(V,I, V(i2),I(i2), '*', V(i3),I(i3), '*')
end;

```

PARAMETERS ESTIMATOR

```
function [Iph, Io, Vt, Rs, Voc]= estimator(Voc_stc, Vmp_stc, Isc_stc, Imp_stc, kv, ki, G, T , adjust_param, VA,VB,VC,IA,IB,IC)
eml.extrinsic('fun');
eml.extrinsic('jac');
% INITIALIZATION
df=ones(3,3);
f=ones(3,1);
T_stc=298;
G_stc=1000;

% INITIAL CONDITION
Vt_stc=(( 2* Vmp_stc - Voc_stc)*(Isc_stc-Imp_stc))/( Imp_stc -(Isc_stc-Imp_stc)*log( (Isc_stc-Imp_stc)/Isc_stc));
Iph_stc=Isc_stc;
Io_stc=Isc_stc/(exp(Voc_stc/Vt_stc)-1);
Rs=(Vt_stc*log((Isc_stc-Imp_stc)/Isc_stc)+Voc_stc-Vmp_stc)/Imp_stc;
% TEMPERATURE AND IRRADIANCE DEPENDENCE
Vt=Vt_stc*T/T_stc;
Isc=Isc_stc *G/G_stc + ki*(T-T_stc);
Iph=Isc;
Voc=Voc_stc+kv*(T-T_stc);
Io=Iph/(exp(Voc/Vt));

%NEWTON-RAPHSON
if adjust_param==1

    y=[Io; Vt;Rs];
    toll=0.5;
    nmax=80;
    f=fun(Iph,y,VA,VB,VC,IA,IB,IC);
    df=jac(y, VA,VB, VC,IA,IB, IC);
    niter=0;
    diff=toll+1;
    while diff>=toll && niter<=nmax
        niter=niter+1;
        diff=-df\f;
        y=y+diff;
        diff=norm(diff);
        f=fun(Iph,y,VA,VB,VC,IA,IB,IC);
        df=jac(y, VA,VB, VC,IA,IB, IC);
    end
% OUTPUT PARAMETERS
Io=y(1);
Vt=y(2);
Rs=y(3);
end
```


References

- [1] V.U. Hoffmann and A. Goetzberge, *Photovoltaic Solar Energy Generation*.
- [2] Solar Magazine, "European Photovoltaic Solar Energy Technology," 2010.
- [3] R.Patel, *Wind and Solar Power Systems*.
- [4] R.Teodorescu, M.Liserre and P.Rodriguez., *Converters for Photovoltaic and Wind Power Systems*. Wiley, .
- [5] D. F. Dunster, *Semiconductors for Engineers*. Business Books, .
- [6] World Energy Council ., "Renewable energy resources: A guide to the future," Kogan Page, .
- [7] Sorensen, *Renewable Energy*.
- [8] E.Lorenzo, *Solar Electricity: Engineering of Photovoltaic Systems*. Progensa, 1994.
- [9] <http://etap.com/renewable-energy/photovoltaic-101.htm>, "Solar Panel Diagram," .
- [10] <http://www.directindustry.com/prod/microsol-international/monocrystalline-photovoltaic-solar-cells-54440-370450.html>, "Monocrystalline-photovoltaic-solar-cells," .
- [11] A.Luque and S. Hegedus, *Handbook of Photovoltaic Science and Engineering*. Wiley, .
- [12] <http://www.pvsolarchina.com/solar-module.html>, "solar module," .
- [13] <http://recyclingtrade.blogspot.dk/2009/03/all-of-pv-solar-cell-module-panel-in.html>, "thin film PV solar module," .
- [14] <http://www.hellotrader.com/energy-development-co-operative/product.html>, "Hybrid solar technology," .
- [15] <http://www.kingspanpowerpanel.com/howpvworks.html>, "Modules, Strings and Array," .
- [16] <http://www.earthkinenergy.com/photovoltaic.html>, "Photovoltaic," .
- [17] http://www.ecosolarenergy.com.au/How_a_Standalone_System_Works-28.htm, "Stand alone photovoltaic systems," .
- [18] <http://www.aes-tunisie.com/en/photovoltaics-grid-connection.php>, "Photovoltaic system connected to the network," .
- [19] Tomas Markvart, *Solar Electricity*. Wiley, 1999.
- [20] S. S. L. Castaner, *Modelling Photovoltaic Systems using Pspice*. Wiley, .
- [21] A. Woyte, J. Nijs, and R. Belmans, *Partial Shadowing of Photovoltaic Arrays with Different System Configurations: Literature Review and Field Test Results*.

- [22] <http://www.civicsolar.com/forum/9824/what-bypass-diode>, "Bypass diode," .
- [23] <http://www.mitsubishielectric.com/bu/solar/faq/index.html>, "Bypassed," .
- [24] R. Ramaprabha and B. L. Mathur, "Characteristics of solar PV array under partial shaded conditions," in *TENCON 2008 - 2008 IEEE Region 10 Conference*, 2008, pp. 1.
- [25] N. Femia, G. Petrone, G. Spagnuolo and M. Vitelli, "Optimization of perturb and observe maximum power point tracking method," *Power Electronics, IEEE Transactions on*, vol. 20, pp. 963, july, 2005.
- [26] C. Pan, J. Chen, C. Chu and Y. Huang, "A fast maximum power point tracker for photovoltaic power systems," in *Industrial Electronics Society, 1999. IECON '99 Proceedings. the 25th Annual Conference of the IEEE*, 1999, pp. 390.
- [27] M. Miyatake, M. Veerachary, F. Toriumi, N. Fujii and H. Ko, "Maximum Power Point Tracking of Multiple Photovoltaic Arrays: A PSO Approach," *Aerospace and Electronic Systems, IEEE Transactions on*, vol. 47, pp. 367, january, 2011.
- [28] D. P. Hohm and M. E. Ropp, "Comparative study of maximum power point tracking algorithms using an experimental, programmable, maximum power point tracking test bed," in *Photovoltaic Specialists Conference, 2000. Conference Record of the Twenty-Eighth IEEE*, 2000, pp. 1699.
- [29] R. Teodorescu and S. Dezso, "Photovoltaic Power Systems in Theory and Practice - Course in Power Systems - Aalborg University," 2011.
- [30] N. Femia, D. Granozio, G. Petrone and M. Vitelli, "Predictive Adaptive MPPT Perturb and Observe Method," *Aerospace and Electronic Systems, IEEE Transactions on*, vol. 43, pp. 934, july, 2007.
- [31] N. Kasa, T. Iida and G. Majumdar, "Robust control for maximum power point tracking in photovoltaic power system," in *Power Conversion Conference, 2002. PCC Osaka 2002. Proceedings of the*, 2002, pp. 827.
- [32] A. wittenmark, *Adaptive Control*. Addison-Wesley, .
- [33] E. Slotine, *Applied Non Linear Control*. Prentice Hall, .
- [34] S. Bittanti, *Identificazione Dei Modelli e Controllo Adattativo*. Pitagora Editrice Bologna, .
- [35] G. A. Vokas, A. V. Machias and J. L. Souflis, "Computer modeling and parameters estimation for solar cells," in *Electrotechnical Conference, 1991. Proceedings., 6th Mediterranean*, 1991, pp. 206.
- [36] A. A. Kulaksiz, "ANFIS-based parameter estimation of one-diode equivalent circuit model of PV modules," in *Computational Intelligence and Informatics (CINTI), 2011 IEEE 12th International Symposium on* Title={ANFIS-Based Parameter Estimation of One-Diode Equivalent Circuit Model of PV Modules}, 2011, pp. 415.

- [37] A. Chatterjee, A. Keyhani and D. Kapoor, "Identification of Photovoltaic Source Models," *Energy Conversion, IEEE Transactions on* Title={Identification of Photovoltaic Source Models}, vol. 26, pp. 883, sept., 2011.
- [38] Miano G., "Differenze finite
," in *Appunti Del Corso Di "Modelli Numerici Per i Campi"* Anonymous 2005, pp. Capitolo 2.
- [39] Bulirsch R. and Stoer J., *Introduction to Numerical Analysis*. Springer, .
- [40] BP Solar, "120-watt multicrystalline photovoltaic module - datasheets and mechanical characteristic," .
- [41] Miano G., "Equazioni non lineari," in *Appunti Del Corso Di "Metodi Numerici Per i Campi"* Anonymous pp. Capitolo 5.